

**STRUCTURAL PERFORMANCES AND FIRE
RESISTING ABILITY OF RUBBERIZED
CONCRETE WALL PANEL UTILIZING
GYPSUM BOARD AS THE SKIN LAYER**

CHEW KAI YUAN

UNIVERSITI TUNKU ABDUL RAHMAN

**STRUCTURAL PERFORMANCES AND FIRE RESISTING ABILITY
OF RUBBERIZED CONCRETE WALL PANEL UTILIZING GYPSUM
BOARD AS THE SKIN LAYER**

CHEW KAI YUAN

**A project report submitted in partial fulfilment of the
requirements for the award of Bachelor of Engineering
(Honours) Civil Engineering**

**Lee Kong Chian Faculty of Engineering and Science
Universiti Tunku Abdul Rahman**

September 2022

DECLARATION

I hereby declare that this project report is based on my original work except for citations and quotations which have been duly acknowledged. I also declare that it has not been previously and concurrently submitted for any other degree or award at UTAR or other institutions.

Signature : 

Name : Chew Kai Yuan

ID No. : 1703767

Date : 07/09/2022

APPROVAL FOR SUBMISSION

I certify that this project report entitled “**STRUCTURAL PERFORMANCES AND FIRE RESISTING ABILITY OF RUBBERIZED CONCRETE WALL PANEL UTILIZING GYPSUM BOARD AS THE SKIN LAYER**” was prepared by **CHEW KAI YUAN** has met the required standard for submission in partial fulfilment of the requirements for the award of Bachelor of Engineering (Honours) Civil Engineering at Universiti Tunku Abdul Rahman.

Approved by,

Signature :



Supervisor : Ts. Dr. Lee Foo Wei

Date : 07/09/2022

Signature :

Co-Supervisor :

Date :

The copyright of this report belongs to the author under the terms of the copyright Act 1987 as qualified by Intellectual Property Policy of Universiti Tunku Abdul Rahman. Due acknowledgement shall always be made of the use of any material contained in, or derived from, this report.

© 2022, Chew Kai Yuan. All right reserved.

ACKNOWLEDGEMENTS

It gives me great pleasure to offer my sincere gratitude to Ts. Dr. Lee Foo Wei, my research supervisor. His commitment, strong enthusiasm, and most importantly, his overpowering attitude, allowed him to assist me in finishing my final-year project. His insightful advice came at the perfect time, and it greatly assisted me in completing this project.

I am extremely grateful to Mr. Lim Zhi Heng, my research mentor for his strong interest in guiding me in the research process. His timely ideas, prompt inspiration, compassion, and dynamism helped me to finish my final year project.

Last but not least, I sincerely appreciate all the helpers who are Jason Ting Jing Cheng, Loh Yong Wei, Ng Kee Siang and Mok Shao Jun for their kind assistance and cooperation throughout the research.

ABSTRACT

Disposal of waste tires is getting severe over the past century as recycling the waste tires is not a common practice. Rubber aggregates produced from waste tires could be used to replace mineral aggregates in concrete wall panels due to their lower unit weight. Such replacement is environmentally sustainable and cost-effective in construction. This study aims to investigate the fire resistance, and structural and thermal performance of the sized-down sandwiched rubberized lightweight foamed concrete (RLFC) wall panel with varying thicknesses of RLFC cores and gypsum board skin layer by conducting flame exposure, thermal conductivity, load bearing, and flexural tests. The gypsum board is used to serve as the sandwiched RLFC wall panel's sheathing material, while the RLFC core with a density of 1150 kg/m^3 is produced to serve as the inner core. The gypsum boards are primarily used to sustain extreme heat while the RLFC core is mainly responsible for supporting the structural load. Epoxy resin is chosen as the connector between the RLFC core and the gypsum boards as it has strong adhesive properties. In the flexural strength test, all the test specimens possessed the same ultimate flexural strength which is 8 kN. However, sandwiched wall panel that utilized 9 mm gypsum board as the skin layer (G9) suffered the largest displacement of vertical deflection which is 6.69 mm in the mid-span among the other specimens. In the load bearing capacity test, G9 possessed the highest load bearing capacity which is 73.6 kN while suffering the largest displacement of lateral deflection which is 1.76 mm. All specimens failed under crushing mode in the load-bearing capacity test. The larger thicknesses of the sheathing materials in the specimens are stiffer to resist the effect of lateral and vertical deflection as well as mitigate the buckling effect. In the thermal conductivity test, G9 outperformed G12 and G16. The thickest RLFC core and lowest density of the gypsum board of G9 enabled it to be the best thermal insulator. In the flame exposure test, the surface conditions of all specimens were similar. The structural integrity as well as the connection between the RLFC core and the gypsum boards were not compromised. This study has proven that the gypsum board provided supreme fire protection and the RLFC core is feasible to be utilized as the inner core of the sandwiched wall panel system due to its high performance in thermal insulation.

TABLE OF CONTENTS

DECLARATION	i
APPROVAL FOR SUBMISSION	ii
ACKNOWLEDGEMENTS	iv
ABSTRACT	v
TABLE OF CONTENTS	vi
LIST OF TABLES	ix
LIST OF FIGURES	x
LIST OF SYMBOLS / ABBREVIATIONS	xiii

CHAPTER

1	INTRODUCTION	1
	1.1 General Introduction	1
	1.2 Significance of the Study	1
	1.3 Problem Statement	3
	1.4 Aim and Objectives	4
	1.5 Scope and Limitation of the Study	4
	1.6 Contribution of the Study	5
	1.7 Outline of the Report	5
2	LITERATURE REVIEW	7
	2.1 Introduction	7
	2.2 Lightweight Concrete	7
	2.2.1 Lightweight Aggregate Concrete	7
	2.2.2 Lightweight Foamed Concrete	11
	2.3 Air Content of Fresh Rubberized Concrete	15
	2.4 Hardened Rubberized Concrete Properties	16
	2.4.1 Water Permeability and Absorption	16
	2.4.2 Density	19
	2.4.3 Flexural Strength	20
	2.4.4 Thermal Conductivity	22

	2.4.5 Fire Performance	23
2.5	Lightweight Sandwich Wall Panel	27
	2.5.1 Gypsum Board as Skin Layer	28
	2.5.2 Epoxy Resin as Connector	29
2.6	Summary	30
3	METHODOLOGY	32
3.1	Introduction	32
3.2	Equipment and Raw Materials	33
	3.2.1 Water	33
	3.2.2 Ordinary Portland Cement (OPC)	33
	3.2.3 Foaming Agent	34
	3.2.4 Fine Aggregates	35
	3.2.5 Crumb Rubber	35
3.3	Specimen Preparation	36
	3.3.1 Formwork	36
	3.3.2 Sieving of Ordinary Portland Cement	37
	3.3.3 Mix Proportions	38
	3.3.4 Mixing Procedure	38
	3.3.5 Density Test	39
	3.3.6 Casting and Curing	40
	3.3.7 Gypsum Board as Sheathing Material	41
	3.3.8 Connection of Gypsum Board to Concrete Core	43
3.4	Laboratory Tests for Sandwich Wall Panel	45
	3.4.1 Load-Bearing Capacity Test	45
	3.4.2 Flexural Strength Test	46
	3.4.3 Flame Exposure Test	47
	3.4.4 Thermal Conductivity Test	48
3.5	Summary	50
4	RESULTS AND DISCUSSION	52
4.1	Introduction	52
4.2	Thermal Conductivity Test	52
4.3	Flame Exposure Test	54
4.4	Flexural Strength Test	55

4.5	Load-Bearing Capacity Test	58
4.6	Summary	63
5	CONCLUSION AND RECOMMENDATIONS	64
5.1	Conclusions	64
5.2	Recommendations	66
	REFERENCES	67

LIST OF TABLES

Table 2.1:	Bulk densities and crushing strengths of the lightweight aggregates (Lo, et al., 2007).	8
Table 2.2:	28-days thermal conductivity of LFC-CM, LFC-PF10 and LFC PF20 (Lim, et al., 2013).	15
Table 2.3:	The air content and slump test of the rubberized concrete mixture (Chylík, et al., 2017).	15
Table 3.1:	3 groups of formworks with different dimensions.	36
Table 3.2:	Mix proportioning of rubberized lightweight foamed concrete.	38
Table 3.3:	Properties of the 9.5 mm gypsum board.	42
Table 3.4:	Properties of the 12 mm gypsum board.	42
Table 3.5:	Properties of the 16 mm gypsum board.	43
Table 3.6:	The details for the dimension of the sized-down sandwich wall panel specimens.	45
Table 4.1:	Thermal conductivity results for each sized down wall panels.	52
Table 4.2:	The result of flame exposure test on the G9 specimen.	54
Table 4.3:	The result of flame exposure test on the G12 specimen.	54
Table 4.4:	The result of flame exposure test on the G16 specimen.	55
Table 4.5:	The result of flexural strength test on the G9 specimen.	56
Table 4.6:	The result of flexural strength test on the G12 specimen.	56
Table 4.7:	The result of flexural strength test on the G16 specimen.	57
Table 4.8:	The result of load-bearing test on the G9 specimen.	59
Table 4.9:	The result of load-bearing test on the G12 specimen.	60
Table 4.10:	The result of load-bearing test on the G16 specimen.	61

LIST OF FIGURES

Figure 2.1:	Crushing strength of lightweight aggregate concretes utilizing 25 mm, 15 mm and 5 mm aggregates (Lo, et al., 2007).	9
Figure 2.2:	The cube strength against the oven-dry density of lightweight aggregate concrete (Newman and Owens, 2003).	10
Figure 2.3:	The thermal conductivity against the density of lightweight aggregate concrete at 3% moisture content (Newman and Owens, 2003).	10
Figure 2.4:	The compressive strength against the density of lightweight foamed concrete (Kozlowski and Kadela, 2018).	12
Figure 2.5:	The flexural strength against the density of lightweight foamed concrete (Kozlowski and Kadela, 2018).	13
Figure 2.6:	The thermal conductivity against the densities of different concrete products (Jonas and McCarthy, 2015).	13
Figure 2.7:	Flexural strength for each type of lightweight foamed concrete (Lim, et al., 2013).	14
Figure 2.8:	Results of water penetration depth test (Li et al., 2019).	17
Figure 2.9:	Results of water absorption test (Ganjian et al., 2009).	18
Figure 2.10:	Results of water permeability depth test (Ganjian et al., 2009).	19
Figure 2.11:	The thermal conductivity against the density of rubberized concrete with 10% error bars (Marie, 2017).	20
Figure 2.12:	Results of the flexural strength test on the specimens (Ganjian et al., 2009).	22
Figure 2.13:	The thermal conductivity against the density of rubberized concrete (Khan and Khitab, 2020).	23
Figure 2.14:	The exposed surface of the concrete specimen with 0% replacement of rubber aggregates after exposure to an extreme temperature of 1000 °C (Hernández-Olivares and Barluenga, 2004).	25
Figure 2.15:	The exposed surface of the concrete specimen with 3% replacement of rubber aggregate after exposure to an	

	extreme temperature of 1000 °C (Hernández-Olivares and Barluenga, 2004).	25
Figure 2.16:	Side view for the curvature of test specimens at different percentages of rubber aggregate replacement after exposure to high temperature (Hernández-Olivares and Barluenga, 2004).	26
Figure 3.1:	Overall workflow of the project.	32
Figure 3.2:	‘Orang Kuat’ branded ordinary Portland cement (OPC).	33
Figure 3.3:	Foaming agent, SikaAER [®] - 50/50.	34
Figure 3.4:	Foam generator.	34
Figure 3.5:	Oven-dried fine aggregate.	35
Figure 3.6:	Powdered crumb rubber.	35
Figure 3.7:	Sawing formworks by using a circular saw.	36
Figure 3.8:	The 3 groups of formworks are prepared.	37
Figure 3.9:	Sieving of ‘Orang Kuat’ branded OPC with 600 µm screen.	38
Figure 3.10:	Mixing procedure of rubberized lightweight foamed concrete.	39
Figure 3.11:	Density test of fresh concrete.	40
Figure 3.12:	Oven-dried concrete cores in a furnace.	41
Figure 3.13:	Resin and hardener.	43
Figure 3.14:	Epoxy resin is being applied to the surface of the concrete core.	44
Figure 3.15:	Sized-down wall panel utilizing gypsum board as skin layer.	44
Figure 3.16:	Set-up of the load-bearing capacity test on vertically positioned sandwiched wall panel.	46
Figure 3.17:	Set-up of the flexural strength test on a sandwiched wall panel.	47
Figure 3.18:	Commencement of flame exposure test on a wall panel specimen.	47

Figure 3.19:	Set-up of the flame exposure test.	48
Figure 3.20:	The specimen is covered with wools before the test.	49
Figure 3.21:	Temperature of hot plated is heated up to 40 °C.	49
Figure 3.22:	Set-up of thermal conductivity testing equipment.	50
Figure 4.1:	The ultimate flexural strength against the displacement of vertical deflection for all specimens.	57
Figure 4.2:	The load-bearing capacity against the displacement of lateral deflection for all specimens.	62

LIST OF SYMBOLS / ABBREVIATIONS

%	Percent
±	Plus/minus
°C	Degree celcius
kg/m^3	Kilogram per cubic metre
mm	Millimetre, 10^{-3} m
W/mK	Watts per meter-Kelvin
μm	Micrometre, 10^{-6} m
B	Average specimen width, mm
CaSO ₄	Calcium sulfate
CO	Carbon monoxide
D	Average specimen depth, mm
G12	Sandwich wall panel utilizing 12 mm gypsum skin layer
G16	Sandwich wall panel utilizing 16 mm gypsum skin layer
G9	Sandwich wall panel utilizing 9 mm gypsum skin layer
H ₂ O	Water
L	Span length, mm
LFC	Lightweight foamed concrete
MPa	Megapascal
OPC	Ordinary Portland cement
P	Maximum Load Applied, N
R	Flexural Strength, MPa
RLFC	Rubberized lightweight foamed concrete
VOCs	Volatile organic compounds

CHAPTER 1

INTRODUCTION

1.1 General Introduction

One of the main environmental concerns in the world is solid waste disposal such as waste tyres. This includes the accumulation of responsible and irresponsible disposal of waste tyres is getting severe over time. As one of the living things on the earth, we need to be environmentally aware of this issue as tyres do not decompose naturally. Therefore, researchers around the world had started to search for good uses for rubber waste tyres. Fortunately, it is possible to integrate rubber aggregate with concrete to form rubberized concrete. In this case, rubber aggregate will replace the natural aggregate in the concrete mixture. Moreover, there are advantages of adding rubber aggregate into concrete. Hernández-Olivares and Barluenga (2004) found that utilizing rubber aggregates in concrete has better fire performance than conventional concrete. However, there are disadvantages to the mechanical properties of concrete such as reduced flexural strength, compressive strength and durability when rubber aggregate is added. The research about rubberized concrete is not a new trend and it has been studied for many years. Numerous studies about rubberized concrete have been conducted to discover the potential beneficial contribution of rubberized concrete to the community. This study aims to assess the load-bearing capacity, flexural strength, fire resistance and thermal conductivity by conducting a load-bearing capacity test, flexural strength test, fire test and thermal conductivity test. Before experimenting, a sandwich wall panel with rubberized concrete as its inner core material and gypsum board as its sheathing material will be produced. The experiment will be conducted by replacing the fine aggregate with a powdered rubber crumb in the concrete mixture.

1.2 Significance of the Study

The outcome of this study presents that the utilization of rubber in concrete can improve both fire performance and thermal insulation. The curvature radius of rubberized concrete is relatively smaller when it is exposed to high temperatures (Hernández-Olivares and Barluenga, 2004). The risk of spalling and crack

development of rubberized concrete are reduced when it is exposed to high temperatures (Li, et al., 2011). However, certain criteria or requirements that cannot be achieved by the conventional concrete for fire serviceability limit state. Thus, the study of rubberized concrete is carried out by utilizing gypsum board as its sheathing material to further enhance its fire-resistance capability. Gypsum board serves as a good fire protection material and it slows down fire spreading in burning progression when a fire breaks out in a building. This will help in reducing the casualties of a fire event by allowing occupants to have more time to escape from a fire event as a gypsum board helps to stop the fire from spreading for some time.

Besides, another environmental concern such as global warming leads to high electrical energy consumption by air conditioner systems to maintain a desired indoor temperature in a building. The utilization of the sandwich wall panel contributes to building energy-saving. It has relatively better thermal insulation and can minimize the energy consumption of buildings and facilities operations by improving energy efficiency and reducing energy loss of the building envelope or walls (Ding, et al., 2013).

In the construction industry, clients prefer the cost of their project to be as minimum as possible. Unfortunately, conventional walls system such as masonry systems is still utilized in constructing a building leading to higher construction costs. This is because a conventional wall system will add more dead load to a building and more reinforcement in structural members is needed to support the load. Therefore, this study of lightweight concrete sandwich wall panels will contribute to the saving cost of construction. The weight of lightweight concrete sandwich wall panels is relatively lower and effectively reduces a structure's dead weight leading to a lower requirement of structural reinforcement (Lakhshmikandhan, et al., 2017).

This study will also help to reduce environmental pollution caused by the accumulation of waste tyres. Non-recyclable wastes such as waste tyres are usually burnt in landfills. Incineration of waste tyres in open areas can release toxic pollutants such as sulfur dioxide, particulates, volatile organic compounds (VOCs) and carbon monoxide (CO). Uncontrolled waste tyre incineration endangers public health and poses an environmental hazard (Shakya, et al., 2006). Furthermore, the accumulation of waste tyres can provide an attractive

breeding ground for pests such as mosquitoes, which can transmit life-threatening diseases to the public such as dengue. Instead of disposing of waste tyres at landfill sites, waste rubber can be used to produce rubberized concrete as an alternative way to recycle waste rubber. This will contribute to environmental sustainability and indirectly improve public health as waste rubber tyres are non-biodegradable and can consume a large amount of valuable landfill space.

1.3 Problem Statement

Accumulation of waste rubber tyres is a global environmental concern. The tyres are non-biodegradable and it is reported that an estimated 1.5 billion waste tyres are disposed of globally each year (Mohajerani, et al., 2020). Waste tyres in stockpiles and landfills can cause the leaching of harmful and toxic chemicals into the environment such as manganese, zinc and iron. Zinc leachate into the soil from waste rubber tyres can poison the groundwater and eventually endanger animals and plants (Gualtieri, et al., 2005).

Furthermore, waste rubber tyres in open areas can catch fire and will release harmful gases such as formaldehyde, Carbon monoxide (CO), acrolein and black carbon into the atmosphere. These toxic gases are all hazardous to our health (Singh, et al., 2015).

According to a study conducted by Alam and Khattak (2015), they reported that normal-weight concrete wall has a higher density than a rubberized concrete wall. This means that the normal weight concrete wall is heavier than the rubberized concrete wall and the normal weight concrete wall will contribute higher dead load in a building, resulting in more unnecessary steel reinforcement in structural members and foundations. More unnecessary reinforcement in structural members and foundations will lead to higher and unnecessary costs. Moreover, a wall built using a traditional masonry technique adds more dead load to the building (Lakshmikandhan, et al., 2017).

Moreover, huge energy consumption in buildings caused by global warming is one of the global energy concerns. In a region where the temperature is high, the outdoor temperature may exceed 35 °C. When the exterior surface of a building is exposed to direct sunlight, the temperature of its external wall surface and roof can reach 60 °C or higher (Zhou, et al., 2014). As a result, the

air conditioning system in the building will consume a significant amount of electrical energy to maintain the desired indoor temperature. In the year 2010, 46.6% of building energy was used for maintaining the required indoor temperature in the United States, which consumed the highest amount of building energy (Zhou, et al., 2014). Therefore, a better thermal insulating building envelope such as a wall panel is needed to reduce undesired heat transfer between the external and internal environments to minimize the electricity consumption of the air-conditioning system.

Therefore, the research study of using rubber in lightweight foamed concrete and using gypsum board as its sheathing material is proposed to solve the environmental and hazard concerns as well as optimize the overall cost of a building.

1.4 Aim and Objectives

The aim of this research is to investigate the effects of utilizing rubber aggregates in lightweight foamed concrete with varying thicknesses of the concrete cores and gypsum board as its sheathing material. The objectives for the research are stated below:

- 1) To evaluate the structural reliability of sandwiched rubberized lightweight foamed concrete wall panels in terms of buckling performance by conducting a load-bearing capacity test.
- 2) To investigate the flexural strength of sandwiched rubberized lightweight foamed concrete wall panels.
- 3) To assess the fire performance and thermal conductivity of sandwiched rubberized lightweight foamed concrete wall panels.

1.5 Scope and Limitation of the Study

The scope of this research is stated as follows: Firstly, the effect of rubber aggregate utilization on concrete is investigated. Secondly, to make a comparison between the sized down sandwiched rubberized lightweight foamed concrete (RLFC) with varying thicknesses of the RLFC core and gypsum boards. The scope of this study includes the evaluation of load-bearing performance, flexural strength, thermal conductivity and fire performance of the sized-down sandwiched RLFC specimens.

For the limitation of the study, preparing a set of powdered rubber crumbs of uniform size is extremely difficult. As the rubber aggregates are prepared by a human being, there will be a dimensional error in the rubber aggregates.

1.6 Contribution of the Study

This research highlights the practicality of the sandwiched wall panels utilizing gypsum board as the sheathing materials and rubberized lightweight foamed concrete (RLFC) as the inner core. Moreover, this study encourages the use of waste rubber from used tires as a concrete mix. This sustainable concrete production could reduce the number of disposed waste tires on our mother earth. Additionally, the flame exposure, load-bearing and load-deflection test are the main tests conducted to assess the practicality of sized down sandwiched RLFC wall panels integrating gypsum board as the sheathing materials and RLFC as the inner core in terms of structural and serviceability performance. Furthermore, this study can also be used as a reference for future research in the field to support the development of better and more sustainable wall panel systems in providing supreme thermal insulation and fire protection, as well as to promote green building materials and green technology in the construction sector.

1.7 Outline of the Report

There are five chapters included in this report for this study:

Chapter 1 discusses the introduction for this study, the significance of the study, the problem statement, the aim and objectives of this research as well as the contribution of this study.

Chapter 2 is the literature review of this study which consists of the previous findings and insights on rubberized concrete, lightweight foamed concrete, epoxy resin and gypsum boards from the researchers. The information was obtained from journals and research articles published by professionals.

Chapter 3 is the methodology that discusses the raw materials required for the production of sized-down wall panels, the step-by-step casting procedure of the rubberized lightweight foamed concrete (RLFC) with the relevant mix proportions and the methods of producing sized-down sandwiched wall panels.

Moreover, the types of tests and the methods of conducting the tests are discussed in this chapter as well.

Chapter 4 is the presentation of the results obtained from the tests. A detailed discussion and analysis are made by comparing the results obtained from the tests on the sandwiched RLFC wall panels with various thicknesses of RLFC cores and gypsum boards of the sized down wall panels.

Chapter 5 is the conclusion of the study and it concludes the overall study based on the aim and objectives of this research. Furthermore, several recommendations are proposed for further research.

CHAPTER 2

LITERATURE REVIEW

2.1 Introduction

This chapter presents an overview of the papers that have been published by researchers concerning the report's aim and objectives. The types of lightweight concrete were reviewed in terms of their concrete strength, density, flexural strength and thermal conductivity. The air content of fresh rubberized concrete was explained. Furthermore, the hardened rubberized concrete properties were explained in terms of the water permeability and absorption, density, flexural strength, thermal conductivity and fire performance. Finally, the lightweight sandwich wall panel was discussed in terms of the gypsum board as the sheathing material and epoxy resin as the connector of the wall panel and the sheathing materials.

2.2 Lightweight Concrete

Lightweight concrete saves construction costs, eases construction works, and is an environmentally friendly building material. The weight and weather resistance of lightweight concrete contribute to its potency (Agrawal, et al., 2021). According to Agrawal, et al., (2021), reduction in structural dead load, reduction in structural steel quantity, reduction in foundation sizes, reduction in overall construction cost, lower thermal conductivity, improved fire resistance, heat and sound insulation are all major benefits of lightweight concrete. Rahman, et al., (2018) reported that lightweight concrete is 23 to 80 percent lower in weight than normal-weight concrete, with a dry density ranging from 300 kg/m^3 to 1840 kg/m^3 . There are 2 types of lightweight concrete are discussed in this chapter, namely lightweight foamed concrete and lightweight aggregate concrete.

2.2.1 Lightweight Aggregate Concrete

Lightweight aggregate such as expanded clays, shales, pumice and perlite is used in lightweight aggregate concrete today (Agrawal, et al., 2021). There are two types of lightweight aggregates, namely lightweight fine aggregate and

lightweight coarse aggregate. Lightweight coarse aggregate has a diameter of more than 5 mm and a bulk density of less than 1000 kg/m^3 whereas lightweight fine aggregate has a diameter of less than 5 mm and a bulk density of less than 1200 kg/m^3 . Lightweight aggregate in the concrete is characterized by its high internal porosity, which leads to a low specific gravity (Chi, et al., 2003). Lightweight aggregate concrete has been used in a variety of structural applications, including long-span bridges and offshore platform structures. (Lo, et al., 2004).

The lightweight aggregate's crushing strength determined the crushing strength of lightweight aggregate concrete (Lo, et al., 2007). Lo, et al., (2007) found that the crushing strength of aggregates is not proportional to the aggregate size (diameter), but it is proportional to the aggregate density as shown in Table 2.1.

Table 2.1: Bulk densities and crushing strengths of the lightweight aggregates (Lo, et al., 2007).

Crushing strengths and bulk densities of the lightweight aggregates

Lightweight aggregate (mm)	Bulk density (kg/m^3)	Aggregate strength (MPa)
5	620	4.27
15	830	5.79
25	440	1.69

Therefore, the crushing strength of the lightweight aggregate concrete was increased when the lightweight aggregate's crushing strength was increased.

The concrete strength for lightweight aggregate concrete utilizing 15 mm lightweight aggregates and a water/cement ratio of 0.4 was increased to 37.9 MPa at 7 days, 43.8 MPa at 28 days and eventually increased to 46.6 MPa at 56 days as shown in Figure 2.1.

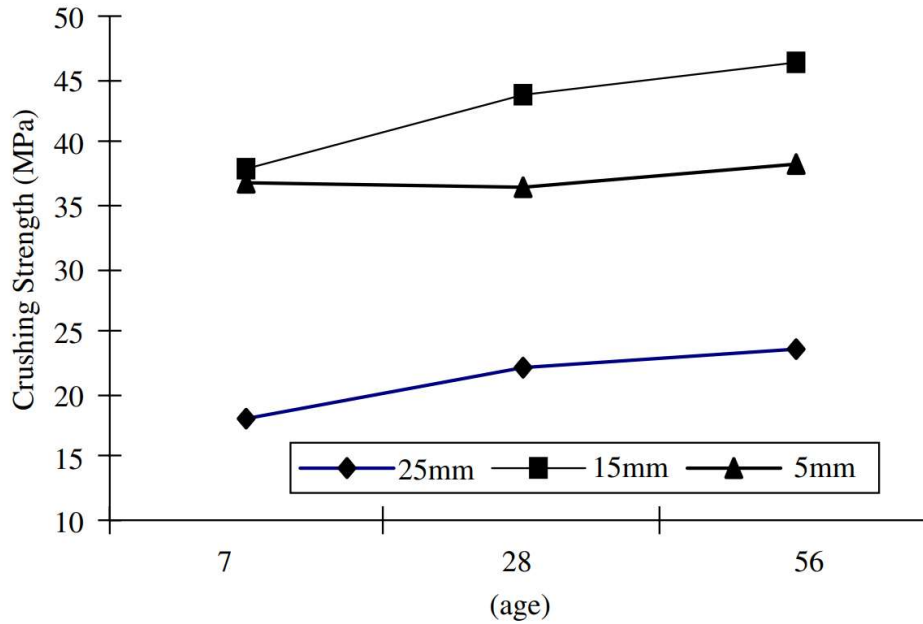


Figure 2.1: Crushing strength of lightweight aggregate concretes utilizing 25 mm, 15 mm and 5 mm aggregates (Lo, et al., 2007).

According to Lo, et al., (2007), the further increment of crushing strength of the concrete from 28 days to 56 days was due to the interfacial zone in the concrete. This is because lightweight aggregate concrete was porous and had higher water absorption than normal-weight concrete, the lightweight aggregate concrete started a self-curing function in the interfacial zone (Lo, et al., 2007). Also, Lo, et al., (2004) found that the 28-day flexural strength of lightweight aggregate concrete ranging from 3.46 MPa to 4.56 MPa had a similar flexural/compressive strength ratio to normal-weight concrete.

In another study conducted by Newman and Owens (2003), the researchers found that the lightweight aggregate concrete with an oven-dry density ranging from 1200 kg/m³ to 2000 kg/m³ was lower than the density of normal-weight concrete ranging from 2300 to 2500 kg/m³. As shown in Figure 2.2, the cube strength of lightweight aggregate concrete was increased when its oven-dry density was increased.

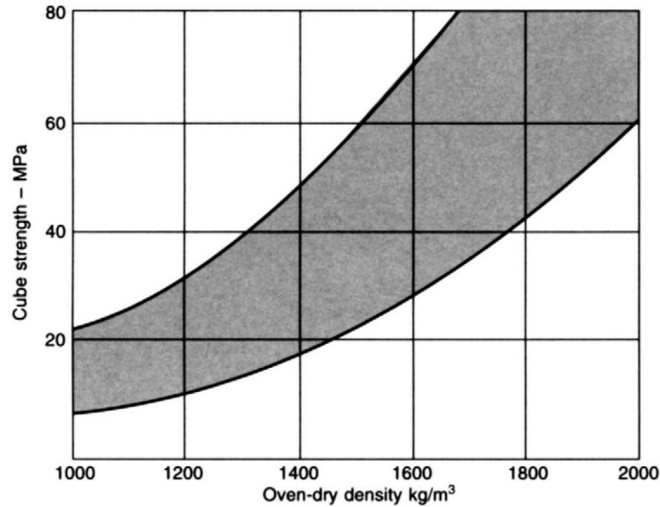


Figure 2.2: The cube strength against the oven-dry density of lightweight aggregate concrete (Newman and Owens, 2003).

Besides, the researchers also found that lightweight aggregate concrete had good thermal insulation. This is because the presence of air in the cellular structure of lightweight aggregate in the concrete helped in reducing the heat rate transfer (Newman and Owens, 2003). As shown in Figure 2.3, the thermal conductivity of lightweight aggregate concrete decreased when its air-dry density was decreased.

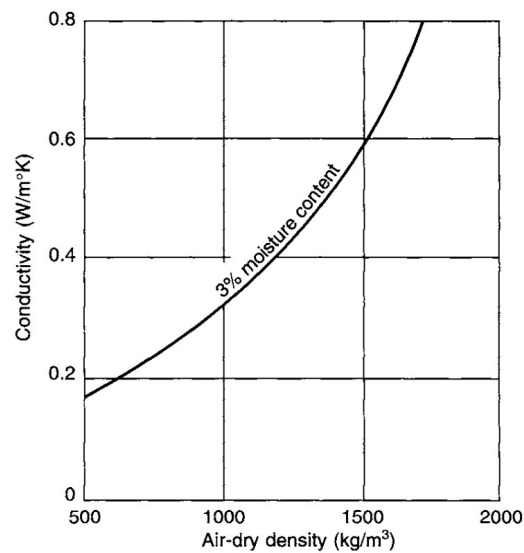


Figure 2.3: The thermal conductivity against the density of lightweight aggregate concrete at 3% moisture content (Newman and Owens, 2003).

Moreover, Newman and Owens (2003) reported that lightweight aggregate concrete with a density of 1600 kg/m^3 and thickness of 175 mm incorporating sintered pulverized fuel ash achieved the same acoustic insulation as a normal-weight concrete wall with the same density and thickness. Furthermore, lightweight concrete aggregate performed better in fire resistance than normal-weight concrete.

2.2.2 Lightweight Foamed Concrete

Lightweight foamed concrete is a cementitious material containing mechanically entrained foam in mortar mix with at least 20 percent by volume, with air pores entrapped in the concrete mixture by using an appropriate foaming agent. Jhatial, et al., (2020) found that the higher the volume of foaming agent used in a concrete mixture, the thermal conductivity and density of lightweight foamed concrete produced were relatively lower. According to a study conducted by Lim, et al., (2013), lightweight foamed concrete has benefits such as low density ranging from 1000 kg/m^3 to 1600 kg/m^3 , improved fire resistance, acoustic and thermal insulation compared to normal-weight concrete. The development of air voids in the lightweight foamed concrete improves thermal insulation by trapping heat absorbed from the exterior and slowing the rate of heat transfer to the interior (Jhatial, et al., 2020). Moreover, utilizing lightweight foamed concrete will have minimal consumption of aggregate (Kozlowski and Kadela, 2018).

Kozlowski and Kadela (2018) reported found that the compressive strength of the lightweight foamed concrete was increased when the density of the concrete was increased as shown in Figure 2.4.

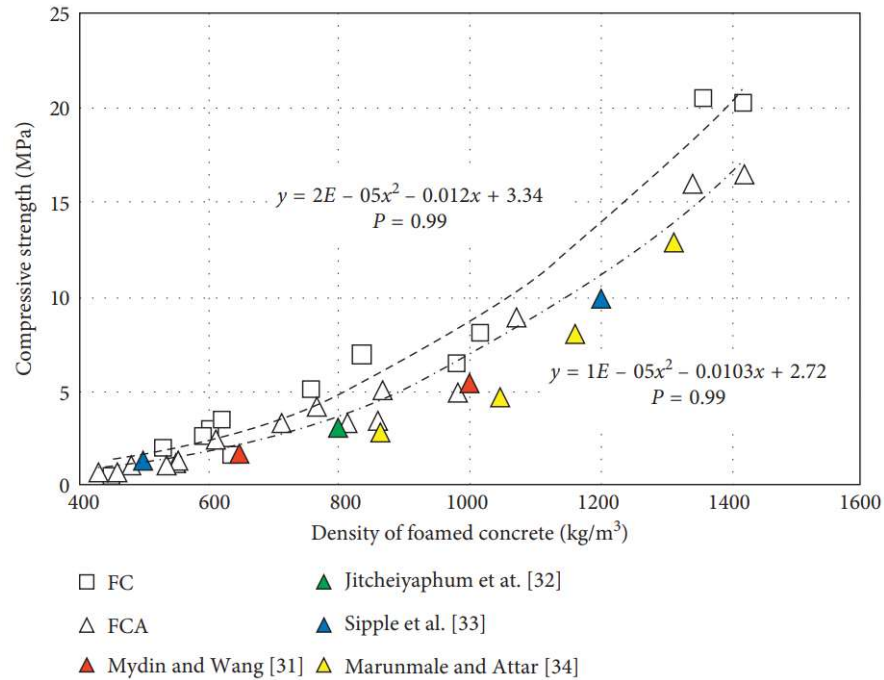


Figure 2.4: The compressive strength against the density of lightweight foamed concrete (Kozłowski and Kadela, 2018).

The density of hardened lightweight foamed concrete was related to the amount of foam content, the composition of cement pastes as well as air voids in the fresh concrete mix. The volume of fresh concrete was increased when there was an increment in foam content. As a result, the density of hardened foamed concrete was reduced and its compressive strength was decreased (Kozłowski and Kadela, 2018). Moreover, the flexural strength of lightweight foamed concrete was found to be decreased when the concrete density was decreased as shown in Figure 2.5.

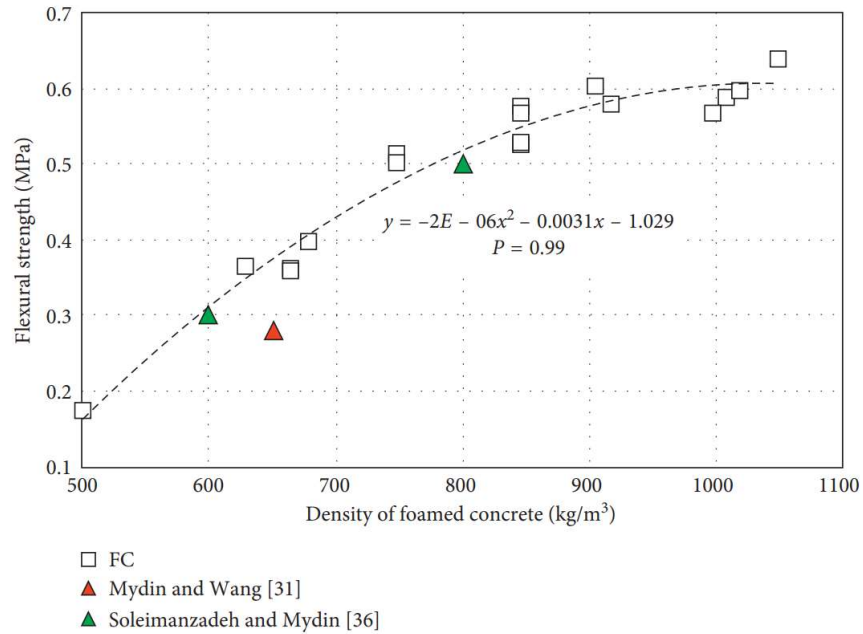


Figure 2.5: The flexural strength against the density of lightweight foamed concrete (Kozłowski and Kadela, 2018).

In a study conducted by Jones and McCarthy (2015), the researchers found that lightweight foamed concrete had low thermal conductivity and excellent thermal insulating properties. As shown in Figure 2.6, the values of thermal conductivity of lightweight foamed concrete ranged from 0.1 to 0.7 W/mK for 600 to 1600 kg/m³ dry densities of the lightweight foamed concrete.

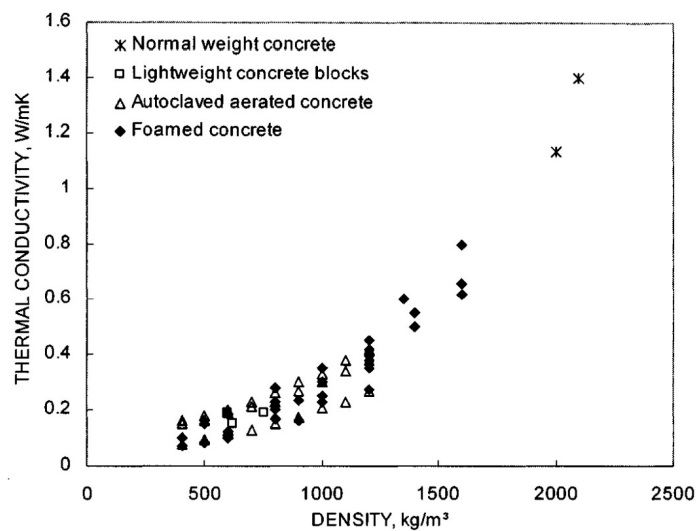


Figure 2.6: The thermal conductivity against the densities of different concrete products (Jonas and McCarthy, 2015).

When the density of the concrete increased, the thermal conductivity of the concrete increased. This showed that lightweight foamed concrete had better thermal insulation than normal-weight concrete as normal-weight concrete had a higher density.

Another research conducted by Lim, et., al (2013) discovered that lightweight foamed concrete containing 10 to 20 percent of palm oil fuel ash had achieved higher flexural strength than lightweight foamed concrete with 100% sand filler. By referring to Figure 2.7, the lightweight foamed concrete incorporating 10% of palm oil fuel ash as a replacement (LFC-PF10) had 25% higher flexural strength than the lightweight foamed concrete incorporating 100% sand filler.

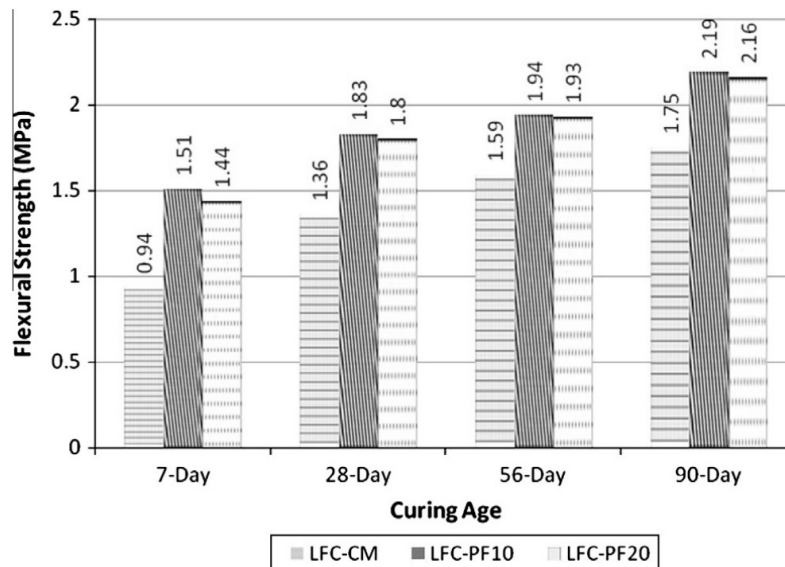


Figure 2.7: Flexural strength for each type of lightweight foamed concrete (Lim, et al., 2013).

Furthermore, the lightweight foamed concrete incorporating 20% of palm oil fuel ash as a replacement (LFC-PF20) had 23% higher flexural strength than the lightweight foamed concrete incorporating 100% sand filler (Lim, et., al, 2013). Moreover, LFC-PF10 and LFC-PF20 had slightly higher thermal conductivity than the lightweight foamed concrete incorporating 100% sand filler as shown in Table 2.2.

Table 2.2: 28-days thermal conductivity of LFC-CM, LFC-PF10 and LFC PF20 (Lim, et al., 2013).

Specimen series No.	28-Day compressive strength (MPa)	Thermal conductivity (W/mk)
LFC-CM-0.56	5.23	0.65
LFC-PF10-0.54	5.62	0.74
LFC-PF20-0.56	5.31	0.67

2.3 Air Content of Fresh Rubberized Concrete

There are numerous studies showed that adding rubber aggregates to a fresh concrete mixture achieved higher air content than a regular concrete mixture without rubber aggregates. Chylík, et al., (2017) reported that adding rubber powder into a fresh concrete mix had caused higher air content in the fresh concrete. The researchers also found that the concrete mix of 40 kg/m³ of rubber powder, 100% of fine rubber/ 0% of coarse rubber (40- RUB- 100/ 0) had higher air content than the other concrete mix comprising 40 kg/m³ of rubber powder and regular concrete mix without incorporating rubber powder (REF) as shown in Table 2.3.

Table 2.3: The air content and slump test of the rubberized concrete mixture (Chylík, et al., 2017).

Mix	Slump [mm]	Air content [%]
REF	70	2.1
40 – RUB - 0/100	35	2.7
40 – RUB - 20/80	45	3.0
40 – RUB - 40/60	35	3.6
40 – RUB - 60/40	28	4.0
40 – RUB - 80/20	16	5.0
40 – RUB - 100/0	25	7.2
80 – RUB - 0/100	---	5.5
80 – RUB - 100/0	---	8.5
120 – RUB - 0/100	---	6.1
120 – RUB - 100/0	---	7.9

According to Chylík, et al., (2017), the surface of the rubber particles captured air molecules when the air molecules penetrated the fresh concrete. Furthermore, fine rubber or powdered rubber had a relatively higher specific surface area, it captured more air molecules than coarse rubber. This is proven

to be accurate by Grinys, et al., (2021), the researchers found that the air content in fresh concrete had increased because of the relatively higher specific surface area of fine crumb rubber or rubber powder than the coarse rubber aggregates. Moreover, the non-polar nature of fine crumb rubber was able to repel water and efficiently entrapped air into concrete (Grinys, et al., 2021). Richardson, et al., (2016) found that more air content was entrapped in the fresh concrete when the fine crumb rubber content was increased. Besides, Muhammad, et al., (2017) also found that the capillarity of the rubber's surface allowed the rubber to entrap higher air content into the fresh concrete mix.

2.4 Hardened Rubberized Concrete Properties

Numerous studies have been done to demonstrate the effect of rubber aggregates in concrete affecting its properties. The affected properties are water permeability, water absorption, density, flexural strength, fire performance and thermal conductivity.

2.4.1 Water Permeability and Absorption

One of the most important aspects in determining the durability of concrete is water permeability. Concrete's durability can be defined as its capacity to withstand abrasion, chemical attack, and weathering while preserving its desired engineering qualities. Reducing the permeability of concrete will increase its resistance to weather conditions such as freezing and thawing cycles, as well as minimize corrosion of concrete and steel bars exposed to acids and minerals.

Several studies have found that the water permeability of concrete was increased when the amount of rubber aggregate replacement in concrete was increased. Research had been conducted by Li, et al., (2019) reported that the water permeability of concrete incorporating rubber aggregates was increased when the content of rubber aggregate was increased. The main factors contributing to the high permeability of concrete containing crumb rubber were porosity and microcracks. The poor bonding between cement pastes and rubber aggregate contributed to the increasing porosity of concrete. The reason behind this was the agglomeration of crumb rubber in concrete had caused weak bonding between rubber aggregate and cement paste in the concrete leading to more microcracks (Li, et al., 2019). The researchers also found that water

penetration depth was increased by up to 225% when crumb rubber replacement in concrete was increased from 2.5% to 20% compared to the control concrete without crumb rubber replacement as shown in Figure 2.8.

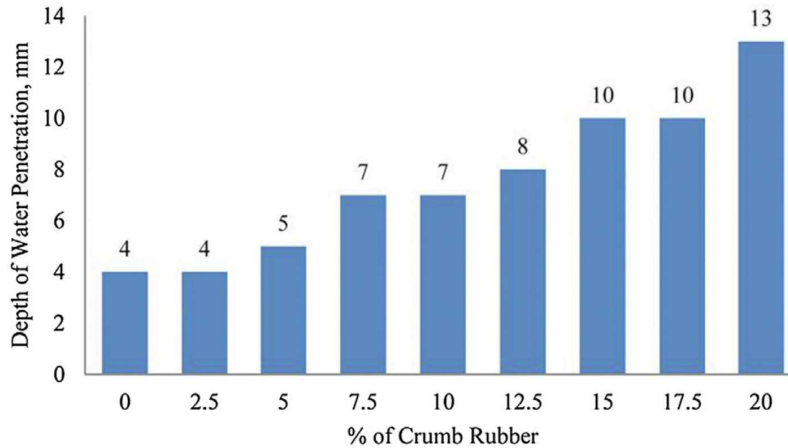


Figure 2.8: Results of water penetration depth test (Li, et al., 2019).

Ganjian, et al., (2009) found that a greater replacement of rubber aggregate in the concrete mixture contributed to a higher water permeability depth of the concrete. They observed that the replacement of chipped rubber for coarse aggregates in concrete led to higher water permeability depth than the replacement of ground rubber for cement in concrete. The water permeability depth of concrete mixtures for both chipped rubber and ground rubber replacements at 5% and 7.5% were categorized as low based on the DIN 1048 standard, whereas the concrete mixtures for both types of rubber replacement at 10% were classified as medium water permeability. The increased permeability of the concrete mixture replaced by ground rubber for cement is caused by a decrease in cement content as well as the weak bonding between the concrete mixture and the rubber aggregates (Ganjian, et al., 2009).

Moreover, another research conducted by Su, et al., (2015) found that water permeability was reduced when rubber particle size was decreased. When the sand in concrete was replaced partially by large rubber particles, the concrete had a lower density than the concrete incorporating smaller or well-graded rubber particles. Furthermore, the concrete that was partially replaced by large rubber particles for sand had more micro-conduits for water to penetrate through. Besides, mixing rubber particles of various sizes into concrete caused the

concrete to be more compact as the smaller rubber aggregates will fill the gaps created by larger rubber aggregates. Therefore, the number of conduits available in concrete for water to travel was decreased (Su, et al., 2015).

For water absorption of rubberized concrete, there are numerous research has found that the increase in the percentage of rubber aggregate replacement in concrete led to higher water absorption of the concrete (Li, et al., 2019). Li, et al., (2019) reported that rubber particles in concrete effectively generated open pores and capillaries that can be filled with water. Therefore, the water absorption of rubberized concrete was greater than the conventional concrete without incorporating rubber aggregates. It was found that the water permeability of concrete was increased when the replacement of rubber aggregates was more than 3%. This was due to poor bonding between cement paste and rubber aggregates in the concrete. (Li, et al., 2019).

Ganjian, et al., (2009) found that using chipped rubber as a replacement for coarse aggregate in concrete had higher water absorption than the concrete that used ground rubber as a replacement for cement. This was discovered when the concretes containing chipped rubber replacement for coarse aggregate formed cracks during oven drying. The cracks were formed in the concrete due to the weaker bond between the larger chipped rubber aggregates and the cement paste than the bonding in the concrete containing ground rubber. Based on Figure 2.9, the water absorption of concrete containing ground rubber replacement for cement was decreased when the percentage of ground rubber replacement for cement was increased.

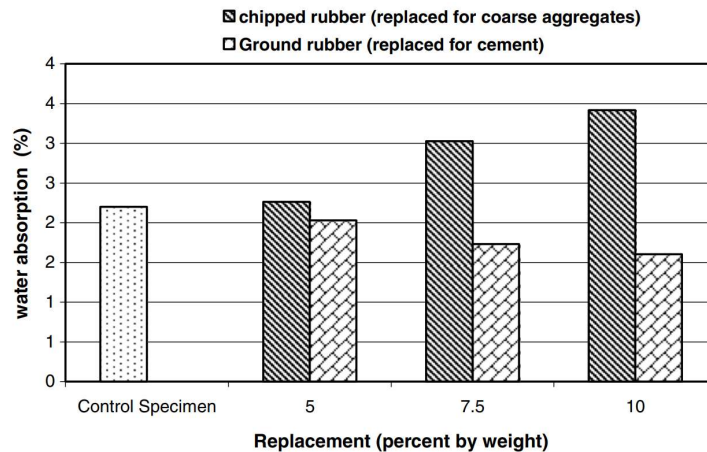


Figure 2.9: Results of water absorption test (Ganjian, et al., 2009).

However, the increasing percentage of ground rubber replacement for cement led to increasing water permeability depth of the concrete incorporating ground rubber as shown in Figure 2.10.

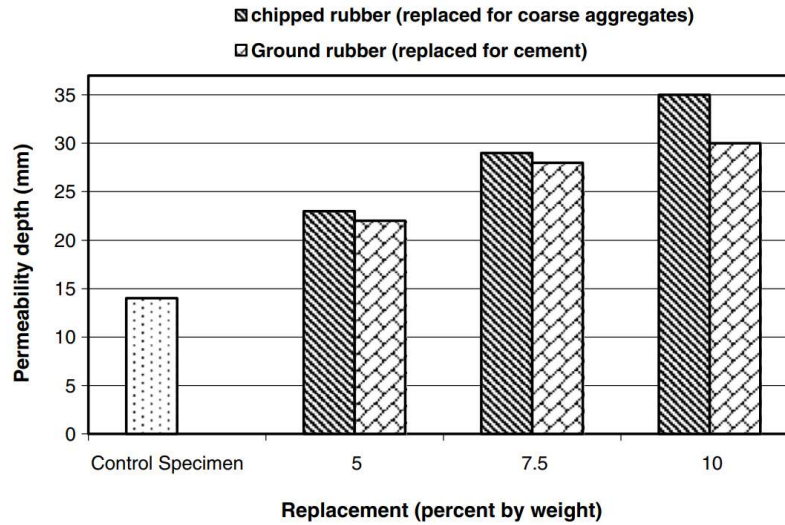


Figure 2.10: Results of water permeability depth test (Ganjian, et al., 2009).

The reason behind the increasing water permeability depth was the presence of capillaries filled with water in the rubberized concrete and a weak bond between the rubber aggregates and cement paste.

2.4.2 Density

A study conducted by Alam and Khattak (2015) reported that rubberized concrete had a lower density than regular concrete without rubber aggregate replacement. The density of concrete was decreased when the replacement of rubber aggregates in the concrete was increased. This was due to the amount of air entrained or trapped in concrete, as well as the water-cement ratio, which was influenced by rubber aggregate size, determined the density of concrete. Therefore, the reduction in the density of concrete was caused by an increase in the amount of air content when the content of rubber aggregates in the concrete was increased (Alam and Khattak, 2015). Another research conducted by Siddiquw and Naik (2004) found that rubber aggregates' non-polar nature tended to entrap air in their rough surfaces. Therefore, the density of concrete decreased when rubber content was increased.

Muhammad, et al., (2017) reported that the dry density of fine aggregate and coarse aggregate was 1552 kg/m^3 and 1679 kg/m^3 respectively. They also found that the dry density for rubber aggregate was 677 kg/m^3 . Moreover, another research done by Marie (2017) found that the thermal conductivity of rubberized concrete decreased when its density was decreased as shown in Figure 2.11.

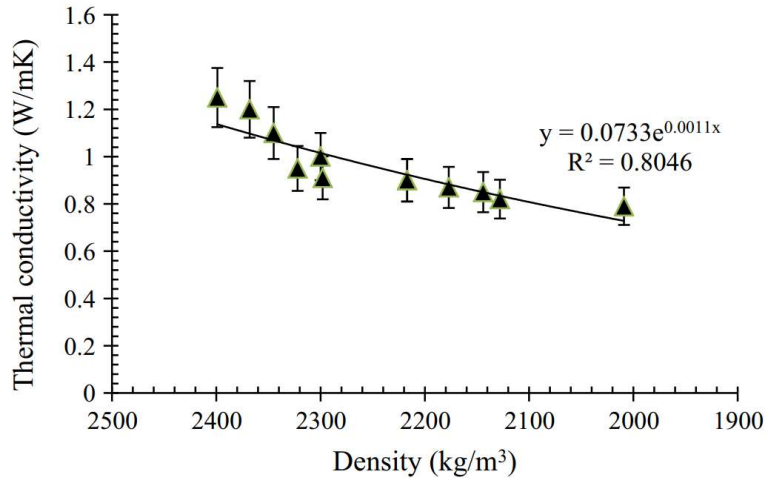


Figure 2.11: The thermal conductivity against the density of rubberized concrete with 10% error bars (Marie, 2017).

The reduction in thermal conductivity of rubberized concrete was caused by the presence of air in the concrete matrix, which resulted in a lower density (Marie, 2017).

2.4.3 Flexural Strength

Flexural strength is a parameter of tensile resistance of a material which is almost the same as tensile strength. The difference between the tensile strength test and flexural strength test is in tensile strength; the highest tensile force is applied to a material's total volume, whereas in flexural strength; the highest tensile force is located at the neutral axis from the bottom edge of the concrete. For the flexural strength test, cracks will be formed at the weakest fiber detected in concrete. If the material is homogenous, its flexural strength is the same as its tensile strength. The flexural strength is usually higher than the tensile strength if a material is not homogenous.

Ganjian, et al., (2009), found that a 10 percent replacement of chipped rubber aggregates for coarse aggregates obtained flexural strength of 3.37 MPa, whereas the replacement of 10 percent of ground rubber for cement in concrete obtained higher flexural strength of 3.80 MPa. The rubberized concrete specimens with rubber aggregate replacements for coarse aggregate and cement were lower in flexural strength compared to the normal-weight concrete with 0 percent rubber aggregate replacement which had a flexural strength of 5.35 MPa. In the first mixture (replacement of chipped rubber for coarse aggregate), there was a 37 percent reduction in flexural strength compared to the control sample. For the second mixture (replacement of ground rubber for cement), there was a 29 percent reduction in flexural strength. The more rubber particles were replaced in a concrete mixture, the lower the flexural strength. The poor bonding between rubber aggregates and the concrete mixture was the main factor in the reduction in flexural strength of the rubberized concrete. The reason was that chipped rubber aggregates can effortlessly be removed from concrete after breaking concrete specimens for the flexural strength test (Ganjian, et al., 2009). The weak bonding was more obvious and weaker in the first mixture, which consisted of chipped rubber aggregates, than in the second mixture, which consisted of powdered rubber (Ganjian, et al., 2009). In this research, it was found that replacing chipped rubber aggregates with up to 5% replacement resulted in the smallest flexural strength loss. However, replacing chipped rubber for coarse aggregate with 7.5% and 10% replacement had a higher reduction in flexural strength than replacing ground rubber for cement with the same percentage of replacement. The reasons for 5% chipped rubber replacement having the least flexural strength reduction, 7.5% and 10% chipped rubber replacement having more flexural strength reduction than ground rubber replacement at the same percentage were not presented by the researchers. These data are shown in Figure 2.12.

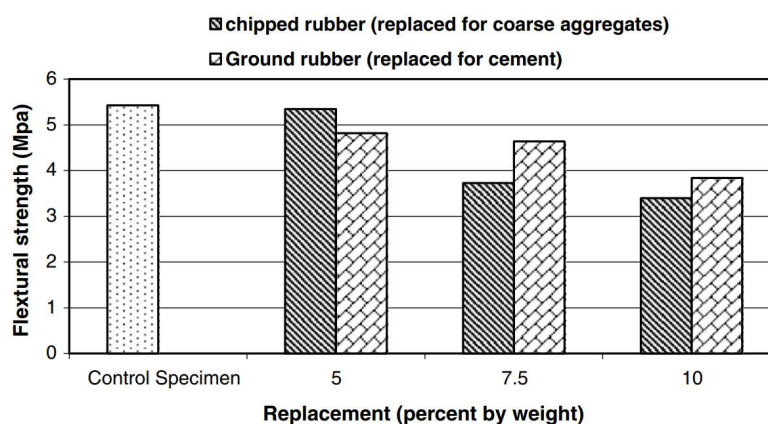


Figure 2.12: Results of the flexural strength test on the specimens (Ganjian, et al., 2009).

Jokar, et al., (2019) found that the flexural strength of concrete utilizing 5% rubber aggregates as a partial replacement for coarse aggregates increased by 25% in comparison to concrete without rubber aggregates replacement. However, the flexural strength was reduced by 9% and 19% respectively when 10% and 15% of coarse aggregates had been replaced by rubber aggregate in concrete mixtures (Jokar, et al., 2019). Moreover, Jokar, et al., (2019) found that the flexural strength of concrete containing rubber aggregates can be enhanced by adding zeolite. The flexural strength can be increased up to 6.34 MPa which was improved by 33% in comparison to the concrete without rubber replacement by adding 10 percent of zeolite to concrete containing 5% of crumb rubber.

2.4.4 Thermal Conductivity

A study conducted by Khan and Khitab (2020) reported that the thermal conductivity of rubberized concrete can be lowered by 30% by replacing 15% of the sand with rubber aggregates. The reduction in rubberized concrete's thermal conductivity was caused by an increase in void content as well as rubber's lower thermal conductivity than sand. The researchers also found that the value of thermal conductivity of air was 0.0026 W/mK, which helped to improve the thermal insulation properties of the specimen. Moreover, rubber's thermal conductivity value ranged from 0.05-0.13 W/mK for particle sizes ranging from 1 to 12 mm. The overall thermal conductivity of rubberized

concrete was decreased when rubber particles replaced sand, which sand had a higher thermal conductivity (Khan and Khitab, 2020). The thermal conductivity and density of rubberized concrete were reduced as the rubber aggregate replacement was increased as shown in Figure 2.13.

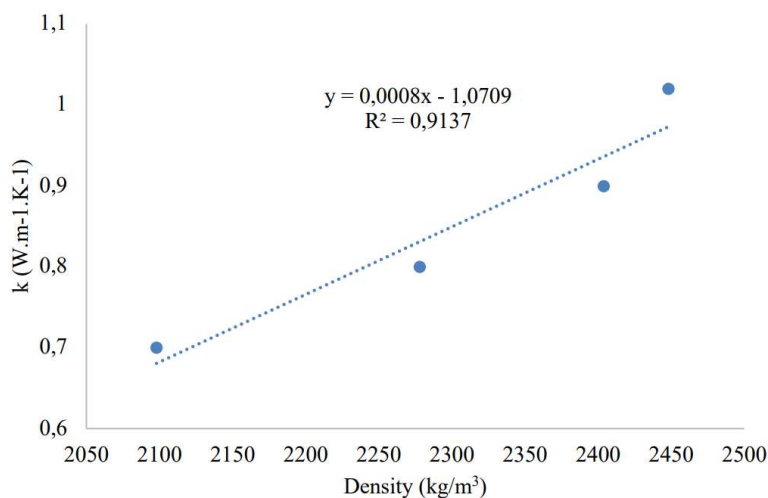


Figure 2.13: The thermal conductivity against the density of rubberized concrete (Khan and Khitab, 2020).

This study had also proven to be accurate by Fadiel, et al., (2014), the researchers found that the poorer thermal conductivity of rubber aggregates than cement mortar matrix caused the reduction in thermal conductivity of rubberized concrete. Moreover, Fadiel, et al., (2014) found that the values of thermal conductivity for rubberized concrete were reduced when the number of rubber aggregates in cement mortar was increased. The heat transmission capability of rubberized concrete was lower than the capability of normal-weight concrete (Marie, 2017).

2.4.5 Fire Performance

There is numerous research has been done on the fire performance of rubberized concrete. Simonetti, et al., (2021) found that rubberized concrete showed signs of spalling when exposed to high temperatures. Rubber concrete in which rubber particles were used as a partial replacement for fine aggregate at a volume ratio of 5 percent (RUB5%) had shown signs of spalling in a minor degree located at its upper and bottom panel surface. For rubber concrete in which rubber particles

were used as a partial replacement for fine aggregate at a volume ratio of 10 percent (RUB10%), severe and explosive concrete spalling was observed at the surface of the upper and bottom panels. On the other hand, conventional concrete panels without rubber replacement showed no sign of spalling. Spalling in rubber concrete was due to the breakdown of recycled rubber aggregates, which happened at around 380°C as an essential attribute of the rubber, as confirmed by other researchers' thermal examination of this material. In this study, the main events and time of main event occurrence were recorded during the experiment. According to Simonetti, et al., (2021), RUB5% panels fulfilled structural stability and integrity standards for 240 minutes but failed to meet thermal insulation parameters at 122.5 minutes when the panels were evaluated by using thermocouple individual temperature, whereas RUB10% panels fulfilled the structural stability requirement for 200 minutes but failed the thermal insulation requirement at 69.5 minutes when evaluated by using thermocouple individual temperature and there was a loss of integrity at 200 minutes. Besides that, dark smoke was produced from both RUB5% and RUB10% when the rubberized concrete specimens had been burnt at a high temperature (Simonetti, et al., 2021).

In another study, Hernández-Olivares and Barluenga (2004) reported that a concrete mixture specimen with rubber aggregate replacement had a greater fire performance when compared to a concrete specimen without incorporating rubber aggregate. It was found that concrete specimens with 0 percent of rubber aggregate replacement showed signs of explosive spalling, whereas specimens with 3%, 5% and 8% of rubber aggregate replacement showed no signs of spalling when the concrete specimens were exposed to an extreme temperature of 1000 °C. The exposed surface of the specimens was shown in Figure 2.14 and Figure 2.15.

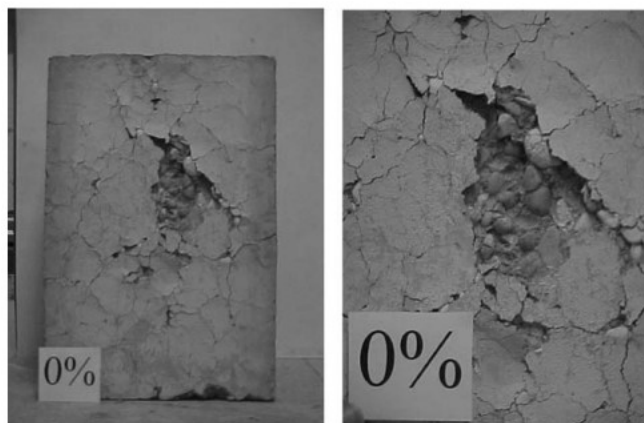


Figure 2.14: The exposed surface of the concrete specimen with 0% replacement of rubber aggregates after exposure to an extreme temperature of 1000 °C (Hernández-Olivares and Barluenga, 2004).

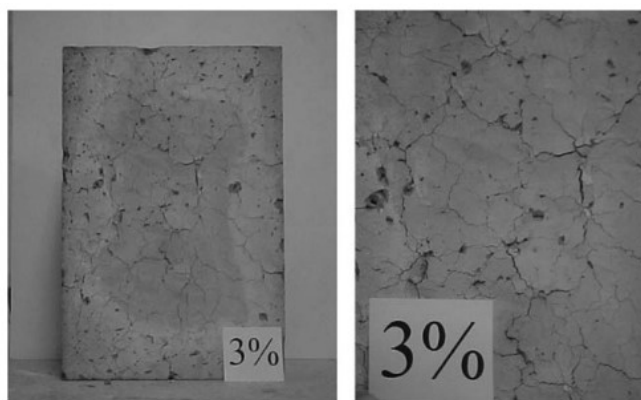


Figure 2.15: The exposed surface of the concrete specimen with 3% replacement of rubber aggregate after exposure to an extreme temperature of 1000 °C (Hernández-Olivares and Barluenga, 2004).

There is a conflict between these two studies conducted by Simonetti, et al., (2021) as well as Hernández-Olivares and Barluenga (2004) about the spalling results of rubberized concrete specimens. Nevertheless, Li, et al., (2011) concluded that the occupied internal space in the concrete specimen was released as the rubber decomposed at high temperatures, thus reducing the saturated vapor pressure in the concrete at high temperatures, lowering the risk of spalling and minimizing crack development. When the amount of rubber

aggregate in the concrete was higher, however, the rubber particles occupied so much interior space inside the concrete that it significantly reduced the essential character of the initial structure as it had broken down, making crack formation and spalling more difficult to avoid. This study conducted by Li, et al., (2011) explained the conflict between the two studies conducted by Hernández-Olivares and Barluenga (2004) as well as Simonetti, et al., (2021), about the spalling results of rubberized concrete specimens.

Other than that, Hernández-Olivares and Barluenga (2004) found that there was a different degree of curvature that happened to the concrete specimens after the specimens were exposed to an extreme temperature of 1000 °C as shown in Figure 2.16.

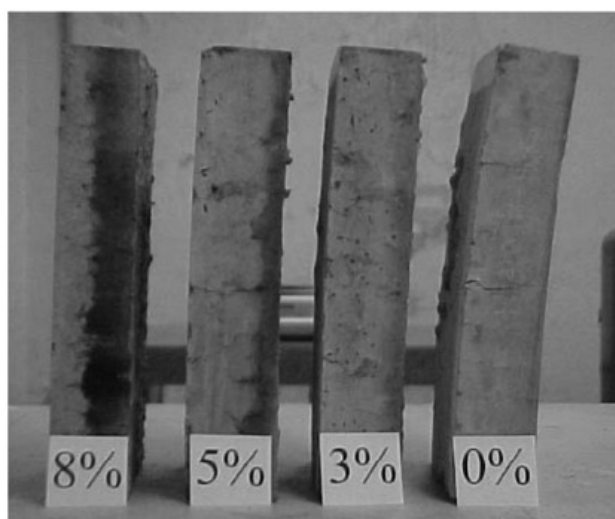


Figure 2.16: Side view for the curvature of test specimens at different percentages of rubber aggregate replacement after exposure to high temperature (Hernández-Olivares and Barluenga, 2004).

Hernández-Olivares and Barluenga (2004) concluded that the relationship between the percentage of rubber aggregate replacement and curvature-radius of the concrete specimens was linear. Concrete specimen with no rubber aggregate replacement was observed to have the largest curvature-radius among the other 3 rubberized concrete specimens, whereas 8% of rubber aggregate replacement in the concrete specimen was observed to have the smallest curvature-radius.

Besides that, Abdullah, et al., (2018) found that the mass loss of rubberized concrete was increased when rubber aggregate replacement and the temperature was increased. The reason was the evaporation of rubber aggregates in rubberized concrete specimens occurred simultaneously at a temperature above 260 °C. Thus, both the density and mass of rubberized concrete were decreased as a result of the evaporation.

2.5 Lightweight Sandwich Wall Panel

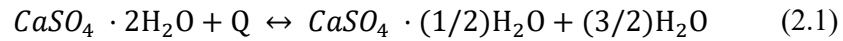
The use of lightweight prefabricated sandwich structural elements in building construction is becoming more popular. A wall built with a traditional masonry technique adds more dead weight to the building. The reduction in the weight of walls will greatly decrease the structure's dead weight and will reduce the sizes of structural components (Lakhshmikandhan, et al., 2017). Therefore, lightweight concrete sandwich wall panels are preferable for wall constructions. A sandwich wall panel consists of at least 2 types of materials. The material of the sandwich wall panel's outer layer is relatively thinner than the inner core material of the wall panel. Sandwich wall panels are divided into two categories. For the first category, the outer skin layer of the wall panel provides thermal and sound insulation, while the inner core of the panel supports the structural load. For the second category, the inner core of the wall panel provides sound and thermal insulation whereas the outer skin layer supports the structural load. Sandwiched wall panels were used to provide thermal insulation to building envelopes to reduce power usage while cooling and heating the interior space of a building (Kumar, et al., 2021).

Bhandari (2016) found that the average density of lightweight sandwich wall panels was 1570 kg/m³ which was relatively less than normal-weight concrete and brick. Therefore, utilizing lightweight sandwich wall panels saves construction costs and building time compared to conventional building methods such as using brick or stone masonry.

Furthermore, the total thickness of composite sandwich wall panels can be reduced by up to one-third of corresponding non-composite wall panels under the same load and span conditions. As a result of the decreased self-weight of composite sandwich wall panels, their seismic performance improved (Kumar, et al., 2021).

2.5.1 Gypsum Board as Skin Layer

Gypsum board is a commonly used construction material, especially in interior design. The main component of the gypsum board is calcium sulfate dihydrate ($\text{CaSO}_4 \cdot 2\text{H}_2\text{O}$). According to a study conducted by Weber (2012), gypsum served as a good fire protection material as it dehydrated at a temperature of about 120 °C. Dehydration contributed as a heat barrier because it was an endothermic chemical reaction that absorbs energy. The study is proven to be accurate by Park, et al., (2009), the researchers found that the presence of water molecules in gypsum was a critical factor in determining gypsum's fire-resistant properties. When crystalline gypsum in gypsum board was heated at a temperature between 125 °C and 225 °C, it dehydrated and released water in vapor form through two separate, reversible chemical reactions as shown in Equation 2.1 and Equation 2.2:



The presence of water in the chemical composition of gypsum helped to improve its thermal insulation (Zhou, et al., 2014).

Zhou, et al., (2014) reported that gypsum's thermal conductivity was lower than conventional concrete. Numerous studies showed that the thermal conductivity of normal-weight concrete was between 1.4 W/mK to 3.6 W/mK. Talebi, et al., (2020) found that the thermal conductivity of normal-weight concrete was between 1.6 W/mK and 3.2 W/mK. Neville and Brooks (2010) also found that the thermal conductivity of normal-weight concrete was between 1.4 W/mK to 3.6 W/mK. Numerous studies showed that the thermal conductivity of the gypsum board was around 0.2 W/mK to 0.28 W/mK at room temperature. Ariyanayagam and Mahendran (2017) found that the thermal conductivity of the gypsum board (density of 812.5 kg/m³) was 0.2 W/mK at room temperature. Wakili, et al., (2006) also found that the thermal conductivity of the gypsum board (density of 810 kg/m³) was 0.28 ± 0.02 W/mK at the temperature of 20 °C.

Research conducted by Chen, et al., (2012) discovered that the calcium silicate boards had explosive spalling while the gypsum board did not have explosive spalling when exposed to high temperatures. As a result, the structural integrity of the calcium silicate board was damaged leading to 20 minutes lesser fire resistance time compared to the gypsum board and it might have caused serious safety accidents. Thus, they recommended not replacing the gypsum board with a calcium silicate board in this case.

Moreover, Yu and Brouwers (2011) reported that the density or porosity of the gypsum board had a significant impact on its thermal conductivity. The thermal conductivity of the gypsum board increased when its density is increased (Yu and Brouwers, 2011). Gypsum is a porous material, the effects of heat transfer through the solid and radiation through the pores in gypsum board are taken into account in determining its thermal conductivity (Rahmanian and Wang, 2012).

2.5.2 Epoxy Resin as Connector

Epoxy resins are synthetic resins made from the reaction of polynuclear phenols, primarily bis-phenol A and epichlorohydrin. Typically, liquid epoxy resins are utilized in the construction industry.

Cheng, et al. (2015) found that a composite sandwich panel that utilized epoxy resin as the connector maintained good stability and no peeling off was observed between the outer layer and the inner core of the sandwich wall panel after conducting the quasi-static localized indentation test. However, a traditional sandwich panel that utilized welding as a connector had its outer panel layer broken away from the core material of the panel. The researchers also found that the energy absorption and energy capacity of the composite sandwich panel that utilized epoxy resin as a connector were greater than the traditional sandwich panel. Similar research had been conducted by Xin, et al. (2019), they found that composite sandwich panels that utilized epoxy resin as a connector had good stability and no detachment between the outer panel layer and the core was observed after the commencement of the drop-weight impact test. This shows that the epoxy resin had high resistance to degradation when it was utilized in the sandwich wall panel as a connector.

Courard (2002) reported that the adhesion of the epoxy resin to a concrete substrate was affected by its surface roughness. Júlio, et al., (2004), found that increasing the surface roughness of concretes through surface treatment resulted in better bonding between the epoxy resin and the concrete. This finding is supported by Courard (2002), it was found that the bonding between the concrete substrate and epoxy resin was improved by increasing the surface roughness of the concrete. The increased surface roughness of the concrete resulted in the improved mechanical interlocking of the adhesion between the concrete substrate and epoxy resin (Courard, 2002).

Furthermore, Ates (2009) reported that epoxy resin solidified at low temperatures without any strain and cracks due to its viscosity. However, the researcher did not explain the reason for how the viscosity of epoxy resin caused its solidification at low temperatures without any strain and cracks. Borri, et al., (2016) found that epoxy resin helped in preventing water-vapor permeability, but it had relatively low fire resistance. Moreover, Chowaniec and Ostrowski (2018) found that the utilization of glass improved the bonding between the concrete substrate and epoxy resin. Besides, Fu, et al., (2014) reported that epoxy resin had a relatively low thermal conductivity.

2.6 Summary

There are two types of lightweight concrete which are Lightweight Aggregate Concrete (LAC) and lightweight foamed concrete. Lightweight Foamed Concrete (LFC) is a cementitious material containing mechanically entrained foam with at least 20 percent by volume in mortar mix. An appropriate foaming agent is used to entrap air pores in the LFC mixture. LFC has a lower density as well as better fire resistance, acoustic and thermal insulation than normal-weight concrete. However, LFC has a lower flexural strength than normal-weight concrete due to the lower density of LFC. There are two types of LAC which are lightweight fine aggregate and lightweight coarse aggregate. Lightweight aggregate in the LAC is characterized by its high internal porosity leading to low specific gravity. LAC has a lower density and better thermal insulation than normal-weight concrete.

A fresh concrete mixture can achieve higher air content by adding rubber aggregates to the concrete mixture due to the surface of the rubber

particles captured air molecules when the air molecules penetrated the fresh concrete. Fine rubber aggregate has a relatively higher specific surface area, it captures more air molecules than coarse rubber aggregate.

Researchers' findings regarding the properties of the hardened concrete are summarized as follows:

- Rubberized concrete has higher water permeability than conventional concrete without rubber replacement due to the higher porosity and microcracks in the rubberized concrete.
- Using chipped rubber as a replacement for coarse aggregate in concrete has higher water absorption than the concrete that used ground rubber as a replacement for cement.
- Rubberized concrete has a lower density than regular concrete without rubber aggregate replacement due to a higher amount of air content or porosity.
- Rubberized concrete has lower flexural strength than normal-weight concrete without rubber aggregate replacement due to the poor bonding between rubber aggregates and the concrete mixture.
- Adding 10% of zeolite to concrete containing 5% of crumb rubber can improve the flexural strength of the rubberized concrete by up to 33% in comparison to the concrete without rubber replacement.
- The thermal conductivity of rubberized concrete is lower than conventional concrete due to the higher void content in rubberized concrete as well as lower rubber thermal conductivity than aggregates.
- The fire performance of rubberized concrete has a better fire performance than conventional concrete as the rubberized concrete shows no signs of spalling and has a smaller curvature radius after exposure to high temperature in comparison to concrete without rubber replacement.

Gypsum board is a construction material and it is good for fire protection as it dehydrates at a temperature of about 120 °C. Dehydration contributes as a heat barrier because it is an endothermic chemical reaction that absorbs energy. Therefore, the presence of water molecules in gypsum is a critical factor in determining gypsum's fire-resistant properties.

CHAPTER 3

METHODOLOGY

3.1 Introduction

The work plan of the study and the experiment's test procedures for obtaining the desired results are covered in this chapter. The work plan of the study is shown in Figure 3.1.

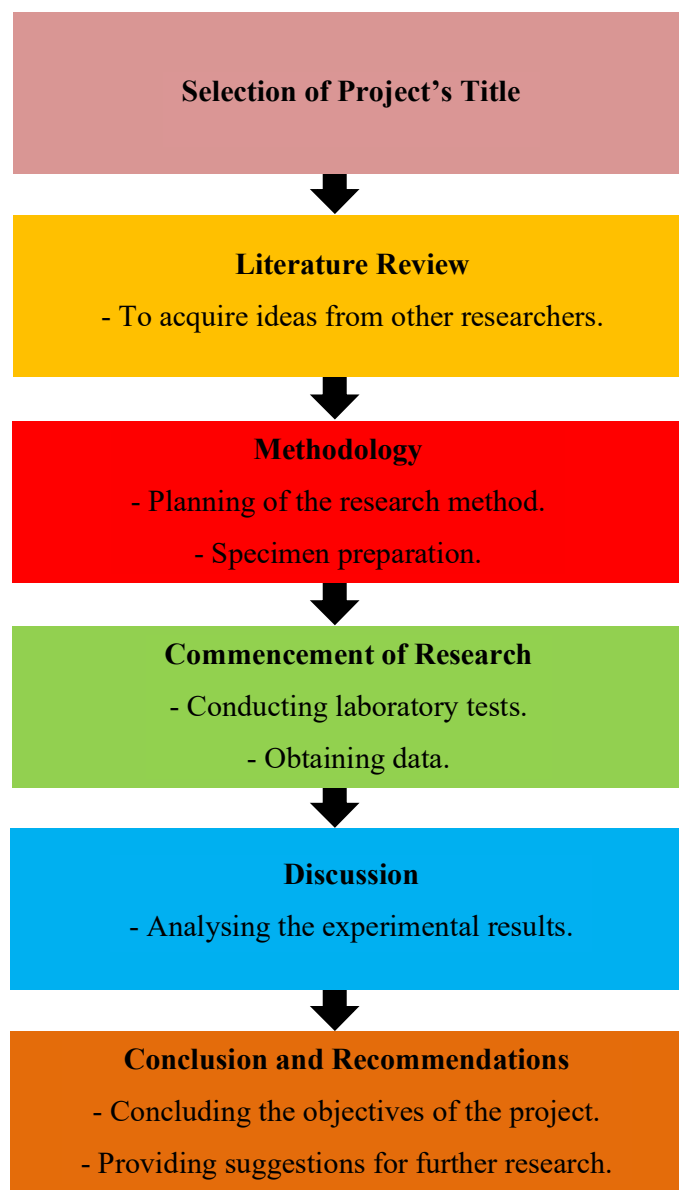


Figure 3.1: Overall workflow of the project.

3.2 Equipment and Raw Materials

The materials used to generate lightweight foamed rubberized concrete to serve as a core of the sandwich wall panel are water, ordinary Portland cement (OPC), foaming agent, fine aggregates and powdered rubber as well as gypsum boards with thicknesses of 9 mm, 12 mm and 16 mm to serve as a sheathing material for the concrete core. The equipment used are flame gun, igniter, type K thermocouple, linear voltage displacement transducer (LVDT), datalogger, hot glue gun, electronic drill gun, circular saw, epoxy resin, plywood, screws, electronic scale, foam generator and furnace.

3.2.1 Water

Water is one of the most significant ingredients in the concrete mix as well as for the concrete curing stage. In accordance with ASTM C1602, tap water is used for concrete mixing in this project. The water-cement ratio used is 0.55 for all testing specimens in this project to standardize the results. The sieved cement is kept in a dry and sealed container to prevent cement from undergoing a hydration process in the presence of humid air.

3.2.2 Ordinary Portland Cement (OPC)

The brand of ordinary Portland cement (OPC) used in the experiment is ‘Orang Kuat’ from YTL Corporation Berhad. The OPC is sieved by using a 600 μm passing sieve to ensure the removal of hydrated clinker from the cement. Figure 3.2 below shows the OPC utilized in the experiment.



Figure 3.2: ‘Orang Kuat’ branded ordinary Portland cement (OPC).

3.2.3 Foaming Agent

The foaming agent, SikaAER[®]-50/50 is used due to its significant air-entraining capabilities. This kind of foaming agent is able to add steady and consistent foam to the concrete mix, avoiding an inaccurate result. To obtain foam with a density of $45 \pm 2 \text{ kg/m}^3$, the foaming agent is diluted with water with the foaming agent to water ratio of 1: 20. Foam is generated with a density of 45 kg/m^3 by pouring the diluted foaming agent into the foam generator with 0.5 MPa operating pressure. Figure 3.3 below shows the foaming agent used in the experiment and Figure 3.4 below shows the foam generator used in the experiment.



Figure 3.3: Foaming agent, SikaAER[®] - 50/50.



Figure 3.4: Foam generator.

3.2.4 Fine Aggregates

Fine aggregates or sand is being used in the concrete mixture during the commencement of the experiment. The moisture content in the sand is removed by oven-drying at 105 °C for 24 hours before using it in the experiment. Figure 3.5 below shows the oven-dried fine aggregate.



Figure 3.5: Oven-dried fine aggregate.

3.2.5 Crumb Rubber

In this experiment, powdered crumb rubber is used to replace fine aggregate in the concrete mixture. The size of powdered crumb rubber is less than 0.420 mm. The powdered crumb rubber is used to replace the fine aggregate partially. The same powdered crumb rubber is used for all testing specimens in this experiment to standardize the results. Figure 3.6 shows the powdered crumb rubber that is used in the experiment.



Figure 3.6: Powdered crumb rubber.

3.3 Specimen Preparation

Load-bearing capacity test, flexural strength test, fire resistance test and thermal conductivity test are carried out in this project. 3 groups of specimens prepared for the project are 300 mm x 300 mm x 75 mm dimension with a gypsum board as its outer layer and rubberized lightweight foamed concrete as its core. Each group of specimens utilized gypsum board as its sheathing material with various thicknesses of 9 mm, 12 mm and 16 mm. For each group of the specimen, four lightweight foamed rubberized concrete cores are prepared with a density of 1150 kg/m³.

3.3.1 Formwork

Since there are 3 groups of specimens that utilized gypsum board as its sheathing material with different thicknesses of 9 mm, 12 mm and 16 mm, three groups of formworks with different dimensions are prepared for the three groups of the specimens as shown in Table 3.1.

Table 3.1: 3 groups of formworks with different dimensions.

Group	Dimension of formwork (mm)	Quantity
1	318 x 318 x 57	4
2	318 x 318 x 51	4
3	318 x 318 x 43	4

The formworks are prepared by using a circular saw as shown in Figure 3.7 below.



Figure 3.7: Sawing formworks by using a circular saw.

Plywood with a thickness of 6 mm is used for the base of the formworks and 9 mm for the sides of the formworks. The formworks are fastened by using screws and an electronic drill gun. The surface dimension of the formworks is 318 mm x 318 mm instead of 300 mm x 300 mm because the offset of the 9 mm thickness of the sides for the formworks is accounted for. Before using the formworks, the formworks are cleaned by using a pressure gun to ensure that there is no remaining in the formwork. Before filling the formworks with fresh concrete, a coat of oil is applied to the formworks to ease demoulding works in the future. Figure 3.8 below shows the prepared 3 groups of formworks for this project.



Figure 3.8: The 3 groups of formworks are prepared.

3.3.2 Sieving of Ordinary Portland Cement

Ordinary Portland cement (OPC) ‘Orang Kuat’ is sieved by using a 600 μm passing sieve to ensure the removal of hydrated clinker from the cement. To prevent hydration from occurring in cement, the cement is kept in an air-tight container. Figure 3.9 below shows the ‘Orang Kuat’ branded OPC is sieved with a 600 μm passing sieve.



Figure 3.9: Sieving of ‘Orang Kuat’ branded OPC with 600 μm screen.

3.3.3 Mix Proportions

In this study, the proportion of powdered crumb rubber to be replaced as fine aggregates is 80 percent. The water-cement ratio will be 0.55. The mix proportion of materials is the same for all specimens to generate a consistent rubberized lightweight foamed concrete core for sandwich wall panels is tabulated in Table 3.2.

Table 3.2: Mix proportioning of rubberized lightweight foamed concrete.

Materials	Mix proportions
Water to cement ratio	0.55
Powdered Crumb rubber proportion (%)	80
Water (kg/m^3)	299.97
Cement (kg/m^3)	545.39
Sand (kg/m^3)	109.08
Powdered Crumb rubber (kg/m^3)	181.11
Foam (kg/m^3)	14.45

3.3.4 Mixing Procedure

In the experiment, the amount of required cement, water, powdered crumb rubber, foam and sand are calculated based on the numbers and dimensions of the specimens and weighted with an electric scale. After that, fine aggregates,

powdered crumb rubber and cement are fed into a concrete mixer to mix the materials thoroughly. When the dry mixture is mixed thoroughly, a weighted amount of water is fed slowly into the mixer to form fresh concrete with a desired water-to-cement ratio of 0.55. Then, the diluted foaming agent will be fed into the foam generator with a foaming agent to water ratio of 1:20. Lastly, the generated foam is added to the concrete mixer to mix with the wet mixture until the density of the wet mixture has reached 1150 kg/m^3 . Figure 3.10 below shows the mixing procedure of the rubberized lightweight foamed concrete.



Figure 3.10: Mixing procedure of rubberized lightweight foamed concrete.

3.3.5 Density Test

After mixing the wet mixture is done, 1 litre of the fresh concrete is extracted from the mixer by using a container to measure its density. The density of fresh concrete is measured on an electronic scale to ensure its density is between 1125 kg/m^3 and 1175 kg/m^3 . Before doing the density test, the weight of the container

used to obtain the fresh concrete is measured first. Excess fresh concrete at the top surface of the container is wiped and compacted for consolidation. After ensuring the top surface of the container is flat, excess fresh concrete on the sides of the container is also cleaned to obtain the most accurate density. Then, the container filled with fresh concrete is weighted and its density is recorded. Figure 3.11 below shows the density test of the fresh concrete.



Figure 3.11: Density test of fresh concrete.

The formula to determine the density of fresh concrete is shown in Equation 3.1.

$$\text{Density} = \frac{\text{Mass}}{\text{Volume}} \quad (3.1)$$

3.3.6 Casting and Curing

When the fresh concrete has reached the desired density between 1125 kg/m^3 and 1175 kg/m^3 , the fresh concrete is poured into the 3 groups of formworks as tabulated in Table 3.1. The fresh concrete is compacted at the corners and sides of the formworks to ensure that there are no empty spaces or gaps at the sides of the concrete when it is hardened. Then, compaction is done for the whole fresh concrete to minimize the voids in the fresh concrete. After that, the fresh concrete in the formworks is smoothed by wiping the top of the formworks to

ensure that the surface of the fresh concrete is smooth and even. The fresh concrete in the formworks is given 24 hours to harden.

After 24 hours have passed, demoulding works are done to obtain the hardened rubberized concrete out from the formworks. The demoulded rubberized lightweight foamed concrete (RLFC) cores are placed in a water tank to cure. The specimens are cured for 28 days to achieve an ideal concrete strength. During the curing process, the temperature of the water tank is controlled between 25 °C and 28 °C.

After 28 days of the curing process, the hardened concrete specimen is taken out from the curing tank and is oven-dried in a furnace at 105 °C for 24 hours to eliminate redundant moisture content in the specimen as shown in Figure 3.12 below.



Figure 3.12: Oven-dried concrete cores in a furnace.

3.3.7 Gypsum Board as Sheathing Material

The gypsum boards are purchased commercially from Knauf Sdn. Bhd. which is formerly known as USG Boral Sdn. Bhd. 3 different thicknesses of gypsum boards purchased are 9.5 mm, 12 mm, and 16 mm.

For the gypsum board with a thickness of 9.5 mm, its density is 557.895 kg/m³ and its edge is tapered. The properties of the 9.5 mm thick gypsum board are shown in Table 3.3 below.

Table 3.3: Properties of the 9.5 mm gypsum board.

Product Name	USG Boral Unispan™		
Size* (mm)	1220 mm X 2440 mm (4' X 8')	Thickness (mm)	9.5
Product Standard	BS EN 520:2004	Weight (kg/m ²)	5.3
Product Testing	BS 476 Part 6 & 7	Edge Detail	Tapered

The product is named USG Boral Unispan and is a lightweight, durable plasterboard that is typically utilized for the internal dry area. The tapered edge of the boards is not utilized, the even surface of the boards is used instead for the preparation of the 9.5 mm thickness gypsum boards as the sheathing material for the concrete cores to prevent the inconsistent surface of the sheathing materials.

For the gypsum board with a thickness of 12 mm, its density is 595.833 kg/m³ and its edge is tapered. The properties of the 12 mm thick gypsum board are shown in Table 3.4 below.

Table 3.4: Properties of the 12 mm gypsum board.

Product Name	USG Boral Basic Board
Thickness (mm)	12
Weight (kg/m ²)	7.15
Size* (mm)	1220 mm X 2440 mm (4' X 8')
Edge Detail	Tapered

The product is named USG Boral Basic Board and is an interior wall and ceiling lining. The tapered edge of the boards is not utilized, the even surface of the boards is used instead for the preparation of the 12 mm thickness gypsum boards as the sheathing material for the concrete cores to prevent the inconsistent surface of the sheathing materials.

The gypsum board with a thickness of 16 mm, its density is 812.5 kg/m³ and it has a square edge instead of the tapered edge. The properties of the gypsum 16 mm thick gypsum board are shown in Table 3.5 below.

Table 3.5: Properties of the 16 mm gypsum board.

Thickness	Metric (mm)	12.5mm, 16mm
Edge Details:	Recessed Edge	Yes
	Square Edge	Yes
Width (mm):	1220	
Length (mm):	2440, 2743, 3048	
Weight:	12.5mm = 10.50kg/m ² , 16mm = 13.00kg/m ²	
Product Testing:	BS 1230 part 1, ASTM C473	

The product is named Boral Firestop and is specifically developed and put through testing for use in fire-rated applications.

3.3.8 Connection of Gypsum Board to Concrete Core

In this experiment, an appropriate adhesive material must be used to connect the gypsum boards to the rubberized lightweight foamed concrete specimen. Therefore, epoxy resin is chosen as the connector of the gypsum boards to the specimen due to its high resistance to degradation and strong adhesive characteristics. Figure 3.13 below shows the resin and hardener used in the experiment.



Figure 3.13: Resin and hardener.

To connect the gypsum boards to the specimen, resin and hardener are mixed with a weight ratio of 3:1 to form an epoxy resin. The epoxy resin is evenly applied with appropriate thickness to the surface of the hardened concrete. Both sides of the concrete core's surface are appropriately applied with epoxy resin for the connection of gypsum boards to produce a 300 mm x 300 mm x 75 mm rubberized lightweight sandwich wall panel as shown in Figure 3.14 below.



Figure 3.14: Epoxy resin is being applied to the surface of the concrete core.

The sandwich wall panel consists of gypsum boards as its outer layer on both sides and rubberized lightweight foamed concrete as its inner core as shown in Figure 3.15 below.



Figure 3.15: Sized-down wall panel utilizing gypsum board as skin layer.

The details of the sized-down sandwich wall panel specimens are summarized in Table 3.6 below.

Table 3.6: The details for the dimension of the sized-down sandwich wall panel specimens.

Specimens	Thickness of concrete core (mm)	Thickness of gypsum board (mm)
G9	57	9
G12	51	12
G16	43	16

3.4 Laboratory Tests for Sandwich Wall Panel

After the sandwich wall panels have been produced, the four tests conducted on the sized-down wall panels with various thicknesses of concrete cores and gypsum layers are the load-bearing capacity test, flexural strength test, fire resistance test and thermal conductivity test.

3.4.1 Load-Bearing Capacity Test

In the load-bearing capacity test, a 300 mm x 300 mm x 75 mm sandwich wall panel is placed vertically as a column with 2 steel plates that are placed on top and bottom of the specimen. A compressive load at a constant rate of 0.5 kN/s is applied to the specimen. 2 linear voltage displacement transducers (LVDT) are used to measure the displacement of lateral buckling deflection of the specimen by installing the LVDTs pointing their tips to the centre of the specimen on both sides. The readings of lateral deflection displacement and applied load at the interval of 5 kN are obtained by using the data logger TDS-530. The load capacity of the specimen is determined by the load at which the specimen starts to crack. The set-up of the load-bearing capacity test on the sandwiched rubberized lightweight foamed concrete (RLFC) wall panels is shown in Figure 3.16.



Figure 3.16: Set-up of the load-bearing capacity test on vertically positioned sandwiched wall panel.

3.4.2 Flexural Strength Test

The flexural test for the sandwich wall panel specimen is conducted under three-point loading. The sandwiched rubberized lightweight foamed concrete (RLFC) wall panel specimen is carefully placed on the midpoint of the supports. The total unsupported span length is set to 25 mm and the effective span length is set to 250 mm. A steel rod is placed in the centre and along the longitudinal axis of the specimen to ensure that load is distributed to the specimen evenly with a constant applied loading rate of 0.5 kN/s. The diameter of the supports and the steel rod is at least 10 mm to prevent local indentation failure on the specimen. The applied load and displacement are recorded by using a data logger TDS-530 when the specimen encountered failure by developing cracks. Equation 3.2 below is used to calculate the sandwiched RLFC wall panels' flexural strength:

$$R = \frac{3PL}{2BD^2} \quad (3.2)$$

where

R = Flexural Strength, MPa

P = Maximum Load Applied Indicated by Compression Machine, N

D = Average specimen depth, mm

L = Span length, mm

B = Average specimen width, mm

The set-up for the flexural strength test on the sandwich wall panel specimen is shown in Figure 3.17 below:



Figure 3.17: Set-up of the flexural strength test on a sandwiched wall panel.

3.4.3 Flame Exposure Test

The flame exposure test for the sandwiched rubberized lightweight foamed concrete (RLFC) wall panel specimen is conducted by exposing one side of the wall panel specimen to a continuous flame at least 600 °C for 60 minutes. A type K thermocouple can measure a temperature range up to 1370 °C and it is stationed at the centre of the specimen without facing the continuous flame as shown in Figure 3.18 below.



Figure 3.18: Commencement of flame exposure test on a wall panel specimen.

During the test, the type K thermocouple is utilized to measure and record the temperature of the exposed surface of the specimen every 10 minutes. When the test is finished, observation for the development of cracks and structural integrity on the sandwiched rubberized lightweight foamed concrete (RLFC) wall panels are done. Figure 3.19 below shows the set-up of the flame exposure test.



Figure 3.19: Set-up of the flame exposure test.

3.4.4 Thermal Conductivity Test

Thermal conductivity measurement equipment is used to conduct the thermal conductivity test. The measurement of steady-state heat flux and thermal transmission properties is conducted in line with ASTM C177. A 300 mm x 300 mm x 75 wall panel specimen is placed between a hot plate which is the heat source and a cold plate. The wall panel specimen is then covered with wool to prevent the heat from escaping directly into the underside of the surface of the cold plate before the commencement of the thermal conductivity test as shown in Figure 3.20.



Figure 3.20: The specimen is covered with wools before the test.

The top side of the specimen and the cold plate is covered with wool as well. The experiment began by raising the temperature of the hot plate up to 40 °C and maintaining the temperature of the cold plate at 26 °C as shown in Figure 3.21 below.



Figure 3.21: Temperature of hot plate is heated up to 40 °C.

The temperature change of both the hot and cold plate assemblies is monitored and recorded every minute by using a CR800 data logger. The hot plate is heated until the temperature reached steady-state heat flux. The thermal conductivity test took 20 hours to complete the experiment. Figure 3.22 below shows the set-up of thermal conductivity testing equipment.



Figure 3.22: Set-up of thermal conductivity testing equipment.

3.5 Summary

Overall, the procedure is separated into two different stages. The first stage is the preparation of formworks for 3 sets of different concrete core thicknesses which are 43, 51 and 57 mm by using a circular saw, drill gun and hot glue gun. Different thicknesses of gypsum boards which are 9, 12 and 16 mm are prepared by using a circular saw to generate 3 sets of 4 sandwiched rubberized lightweight foamed concrete (RLFC) wall panels with the dimension of 300 mm x 300 mm x 75 mm. Next, cement from ordinary Portland cement (OPC) is sieved by using a 600 μm passing sieve before commencing the casting of RLFC wall panels. Next, the powdered rubber, water, sand and cement are weighted before generating the rubberized lightweight foamed concrete by adding the foaming agent, SikaAER[®] - 50/50 to achieve the desired density of 1150 kg/m^3 . To ensure that the density of the fresh concrete is 1150 kg/m^3 , a fresh concrete density test is carried out. The concrete cores are oven-dried at 105 °C for 24 hours to remove excess moisture content after the curing process in a water tank for 28 days. Gypsum boards are installed on both surfaces of the oven-dried RLFC cores by using epoxy resin to generate sandwiched RLFC wall panel with the dimension of 300 mm x 300 mm x 75 mm.

The second stage is the laboratory testing which included a load-bearing test, flexural strength test, flame exposure test and thermal conductivity

test. The tests are conducted on the 300 mm x 300 mm x 75 mm sized down wall panel specimen after the concrete cores are cured for 28 days. The results and observations are recorded for each test and a comparison of the results between the size down wall panel specimen with various thicknesses of concrete cores and gypsum board layers is made.

CHAPTER 4

RESULTS AND DISCUSSION

4.1 Introduction

The performance and behaviour of sized-down sandwiched rubberized lightweight foamed concrete (RLFC) wall panels under load-bearing capacity test, flexural strength test, flame exposure test, and thermal conductivity test are discussed in this chapter. Before proceeding to tests, all concrete samples are cured in a water tank for 28 days. The tests provide insight into the practicality of using gypsum boards as the sheathing materials and RLFC as the inner core of sized-down sandwiched wall panels. The RLFC wall panel specimens with the same dimensions of 300 mm x 300 mm x 75 mm have different thicknesses of RLFC core and gypsum skin layer used for the tests. The analysis and interpretation of the obtained results from the tests are discussed as well.

4.2 Thermal Conductivity Test

The thermal conductivity test is conducted to determine the sized down sandwiched rubberized lightweight foamed concrete (RLFC) wall panel with the lowest and highest thermal conductivity among the specimens with varying thicknesses of RLFC cores and gypsum board skin layers. The thermal conductivity value for each specimen is tabulated in Table 4.1 below:

Table 4.1: Thermal conductivity results for each sized down wall panels.

Specimen	Thermal Conductivity ($\text{Wm}^{-1}\text{K}^{-1}$)
G9	0.4676
G12	0.5481
G16	0.5884

Note:

G9 = Sandwich wall panel utilizing 9 mm gypsum skin layer.

G12 = Sandwich wall panel utilizing 12 mm gypsum skin layer.

G16 = Sandwich wall panel utilizing 16 mm gypsum skin layer.

According to Table 4.1, the thermal conductivity value of the wall panel specimens increases with the increase of gypsum board thickness and the decrease of RLFC core thickness. G9 has the lowest value of thermal conductivity of $0.4676 \text{ Wm}^{-1}\text{K}^{-1}$ whereas G16 has the highest value of thermal conductivity of $0.5884 \text{ Wm}^{-1}\text{K}^{-1}$. The results show that G9 has the best thermal insulation performance among the specimens. This is because G9 has the thickest rubberized lightweight foamed concrete (RLFC) core among the specimens. The air voids and rubber aggregates in the RLFC core improve its thermal insulation by trapping heat energy absorbed from the hot plate and slowing down the rate of heat transfer to the cold plate. Moreover, the thermal conductivity value for both air void and rubber aggregates in the RLFC core is around $0.0026 \text{ Wm}^{-1}\text{K}^{-1}$ and $0.05 \text{ Wm}^{-1}\text{K}^{-1}$ respectively. The thicker the RLFC core of the specimen, the more air voids and rubber aggregates in the RLFC core across its thickness. Therefore, the rate of heat transfer through the specimens from the hot plate to the cold plate decreases with the increase of RLFC core thickness.

Besides, the density of the gypsum board in G16 is the highest among the specimens. The density of gypsum boards in the specimen increases with the increase of the thickness of gypsum boards. The density of the gypsum board used in G16 is 812.5 kg/m^3 whereas the density of the gypsum board used in G12 and G9 are 595.833 kg/m^3 and 557.895 kg/m^3 respectively. The higher density of the gypsum board has lesser void spaces and this increases the rate of heat transfer through the specimen from the hot plate to the cold plate. Thus, a higher density of gypsum board used in a wall panel increases its thermal conductivity. This explains the reason the thermal conductivity value of the wall panel specimens increases with the increase of gypsum board thickness and the decrease of RLFC core thickness. Based on the results in Table 4.1, G9 is the best thermal insulator among the specimens as it exhibits the lowest value of thermal conductivity. Moreover, the thermal insulation performance of G9 is recommended to be utilized as the non-load bearing wall panel to efficiently insulate the heat from the external to the building's interior space. Based on the results obtained, G9 is proposed as a non-load bearing sandwiched wall panel system for further research.

4.3 Flame Exposure Test

The flame exposure test is conducted to assess the fire performance of each rubberized lightweight foamed concrete (RLFC) wall panel with varying thicknesses of RLFC cores and gypsum board skin layer. Observations on the surface conditions of the specimens and their structural integrity are made after 60 minutes of continuous direct flame exposure at the extreme temperature of 600 °C and above. The surface conditions of each specimen are exhibited in figures which are tabulated in Table 4.2, Table 4.3 and Table 4.4 below:

Table 4.2: The result of flame exposure test on the G9 specimen.

Specimen	The condition of the exposed surface to the flame after conducting the test	Time (min)	Temperature (°C)
G9		0	708
		10	795
		20	716
		30	752
		40	767
		50	716
		60	800

Table 4.3: The result of flame exposure test on the G12 specimen.

Specimen	The condition of the exposed surface to the flame after conducting the test	Time (min)	Temperature (°C)
G12		0	707
		10	756
		20	787
		30	755
		40	840
		50	817
		60	718

Table 4.4: The result of flame exposure test on the G16 specimen.

Specimen	The condition of the exposed surface to the flame after conducting the test	Time (min)	Temperature (°C)
G16		0	677
		10	700
		20	703
		30	726
		40	979
		50	976
		60	975

Based on Table 4.2, Table 4.3 and Table 4.4 above, the effect of the 60 minutes of continuous flame exposure to each specimen are similar. Development of minor cracks on all the surfaces of the specimens is observed. Nevertheless, the developed minor cracks are unable to compromise the structural integrity of the sheathing material which is the gypsum board layer. Moreover, it is observed that the connection between the RLFC core and the sheathing materials is not compromised by continuous direct flame exposure as well. There is no detachment between the sheathing materials and the RLFC core of all specimens after the flame exposure test. All sandwiched RLFC wall panel specimens do not experience structural failure after the flame exposure test. Thus, sandwiched RLFC wall panel specimens utilizing gypsum boards as their sheathing materials have proven their capability in providing effective fire protection against continuous flame exposure at an extreme temperature of 600 °C and above.

4.4 Flexural Strength Test

The flexural strength test is conducted to determine the flexural strength and displacement of vertical deflection for each sized down wall panel with varying thicknesses of rubberized lightweight foamed concrete (RLFC) cores and gypsum board skin layers. The specimens are positioned horizontally for the test and a constant load of 0.5 kN/s is applied until the structural failure of the

specimens occurs. The ultimate flexural strength and the displacement of vertical deflection for each specimen are recorded and tabulated in Table 4.5, Table 4.6 and Table 4.7. The results of the flexural strength test for all the specimens are summarized in Figure 4.1.

Table 4.5: The result of flexural strength test on the G9 specimen.

Specimen	The condition of the specimen at ultimate failure	Load (kN)	Deflection (mm)
G9 Ultimate Flexural Strength: 8 kN		0	0
		1	1.0500
		2	1.8300
		3	2.5500
		4	3.1400
		5	3.8100
		6	4.6600
		7	5.4300
		8	6.6900

Table 4.6: The result of flexural strength test on the G12 specimen.

Specimen	The condition of the specimen at ultimate failure	Load (kN)	Deflection (mm)
G12 Ultimate Flexural Strength: 8 kN		0	0
		1	0.4750
		2	0.7800
		3	1.1700
		4	1.8300
		5	2.3500
		6	2.9150
		7	3.6900
		8	4.7800

Table 4.7: The result of flexural strength test on the G16 specimen.

Specimen	The condition of the specimen at ultimate failure	Load (kN)	Deflection (mm)
G16 Ultimate Flexural Strength: 8 kN		0	0
		1	0.4900
		2	0.5950
		3	0.7100
		4	0.7800
		5	1.1550
		6	1.7850
		7	2.5130
		8	4.0950

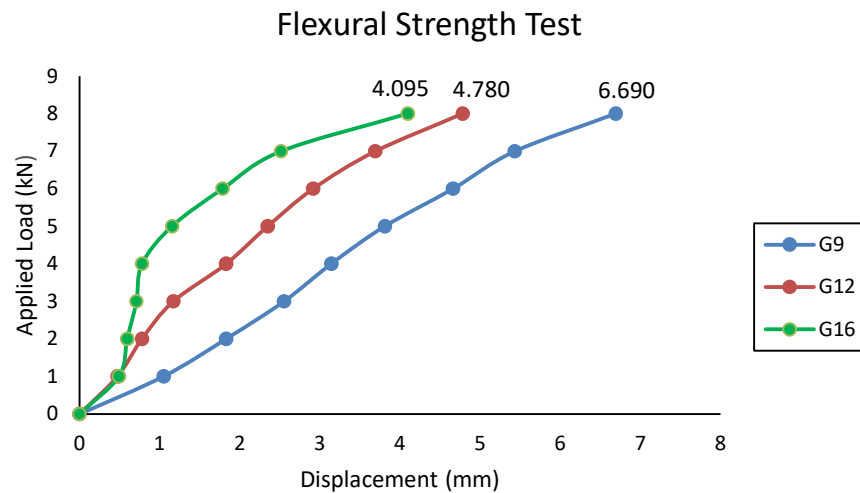


Figure 4.1: The ultimate flexural strength against the displacement of vertical deflection for all specimens.

Based on Figure 4.1, all the sandwiched RLFC wall panels have similar ultimate flexural strength which is 8 kN and experienced shear failure. However, the specimens experienced different magnitudes of displacement in the mid-span caused by the deflection. G16 experienced the least displacement of vertical deflection in the mid-span which is 4.095 mm whereas G9 experienced the

largest displacement of vertical deflection in the mid-span which is 6.69 mm. This is because the thickness of G16's sheathing materials is the thickest and stiffest to be affected by the vertical deflection caused by the constant applied load. The larger the thickness of the sheathing materials for the specimens, the stiffer the sheathing materials resulting in a higher capability of the specimens in resisting the vertical deflection caused by the constant applied load. G9 has the thinnest sheathing materials, it has the least stiffness to resist the deflection caused by the applied load. Therefore, G9 experienced the largest displacement of vertical deflection caused by the constant applied load among the other specimens. Moreover, the sheathing materials of the specimens which are the gypsum boards delayed the development of the major crack in the midspan of the RLFC cores of the specimens. The brittle RLFC cores of the specimens would have ruptured in half at the early loading stage without the flexural strength support provided by the ductile gypsum board.

4.5 Load-Bearing Capacity Test

The load-bearing capacity test is conducted to determine the load-bearing capacity and displacement of lateral deflection for each sized down wall panel with varying thicknesses of rubberized lightweight foamed concrete (RLFC) cores and gypsum board skin layer. The test is conducted after the RLFC core of the specimens had been cured for 28 days. The specimens are positioned vertically for the test and a constant compressive load of 0.5 kN/s is applied until the structural failure of the specimens occurs. The load bearing capacity and the displacement of lateral deflection for each specimen are recorded and tabulated in Table 4.8, Table 4.9 and Table 4.10. The results of the load-bearing capacity test for all the specimens are summarized in Figure 4.2.

Table 4.8: The result of load-bearing test on the G9 specimen.

Specimen	Failure condition	Load (kN)	Lateral deflection, LVDT 1 (mm)	Lateral deflection, LVDT 2 (mm)
G9 Load Bearing Capacity: 73.6 kN Failure mode: Crushing		0	0.0000	0.0000
		5	-0.0600	0.2900
		10	-0.0400	0.3200
		15	-0.0150	0.3700
		20	0.0050	0.3650
		25	0.030	0.3750
		30	0.0500	0.3750
		35	0.0650	0.4650
		40	0.0750	0.5250
		45	0.0900	0.4950
		50	0.0950	0.4850
		55	0.1000	0.4850
		60	0.1050	0.4800
		65	0.1050	0.5200
		70	0.1150	1.2650
73.6	0.1050	1.7600		

Table 4.9: The result of load-bearing test on the G12 specimen.

Specimen	Failure condition	Load (kN)	Lateral deflection, LVDT 1 (mm)	Lateral deflection, LVDT 2 (mm)
G12		0	0.0000	0
		5	-0.1900	0.2350
		10	-0.1750	0.2250
		15	-0.1400	0.2300
		20	-0.1100	0.2350
		25	-0.0900	0.2250
		30	-0.0700	0.2500
		35	-0.0350	0.3000
		40	0.0100	0.3450
		45	0.0400	0.3500
		50	0.1000	0.4250
		55	0.3500	0.3600
		60	0.4400	0.3900
		65	0.5050	0.4700
		70	0.5250	0.6100
73.1	0.5500	0.7950		
Load Bearing Capacity: 73.1 kN				
Failure mode: Crushing				

Table 4.10: The result of load-bearing test on the G16 specimen.

Specimen	Failure condition	Load (kN)	Lateral deflection, LVDT 1 (mm)	Lateral deflection, LVDT 2 (mm)
G16		0	0.0000	0.0000
		5	-0.1950	0.1950
		10	-0.2450	0.2550
		15	-0.2900	0.3050
		20	-0.3300	0.3450
		25	-0.3600	0.3800
		30	-0.3850	0.4150
		35	-0.4100	0.4400
		40	-0.4350	0.4650
		45	-0.4500	0.4850
		50	-0.4600	0.4950
		55	-0.4650	0.5000
		60	-0.4650	0.5000
		65	-0.4600	0.5
		70	-0.4500	0.49
71	-0.4500	0.49		

G16

Load
Bearing
Capacity:
71.0 kNFailure
mode:
Crushing

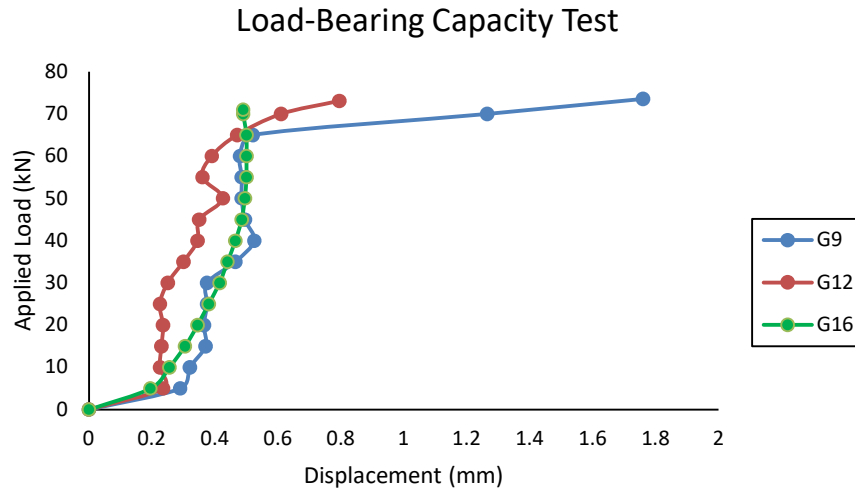


Figure 4.2: The load-bearing capacity against the displacement of lateral deflection for all specimens.

Based on Figure 4.2, G9 has the highest load bearing capacity which is 73.6 kN while having the largest displacement of lateral deflection which is 1.76 mm whereas G16 has the lowest load bearing capacity which is 71.0 kN while having the smallest displacement of lateral deflection which is 0.49 mm. The thicker the RLFC cores of the specimens, the higher the compressive load that the specimen can sustain. Hence, it can be concluded that the RLFC cores of the specimens can sustain a higher compressive load than the gypsum boards. This explains the reason G9 has the highest load-bearing capacity among the other specimens.

G16 has the smallest displacement of lateral deflection as the thickness of its sheathing materials is the largest. This is because a thicker sheathing material is stiffer and is more capable of resisting the lateral deflection caused by the increasing compressive loads. In contrast, G9 has the largest displacement of lateral deflection as the thickness of its sheathing materials is the smallest. This is because the smallest thickness of sheathing materials of G9 is the least stiff to resist the lateral deflection caused by the increasing compressive load.

Moreover, microcracks are observed in the RLFC core and the gypsum board of G16 and are marked with a marker pen after the load-bearing test. G12 and G9 experienced internal structural failure after the test as the equipment

used in the test stopped increasing the compressive load applied to the specimens after it detected an internal structural failure in the specimens. Buckling failure was expected for the specimens in the test. However, all specimens failed under crushing mode. This is because the thicknesses of the gypsum boards used as the sheathing materials in all the specimens are sufficiently large and stiff to mitigate the buckling effect caused by the constant applied compressive load.

4.6 Summary

Overall, the results of the flexural strength, thermal conductivity, load bearing capacity and flame exposure test are presented in this chapter. In the thermal conductivity test, G9 has the lowest value of thermal conductivity of $0.4676 \text{ Wm}^{-1}\text{K}^{-1}$ and is the best thermal insulator among the other specimens. Hence, G9 is recommended to be utilized as the non-load bearing wall panel to efficiently insulate the heat from the external to the building's interior space. In the flame exposure test, the conditions of the surface for all the specimens are similar. Moreover, the connection between the RLFC core and the sheathing materials as well as the structural integrity of the specimens are not compromised by the continuous direct flame exposure. In the flexural strength test, all the specimens possess the same ultimate flexural strength which is 8 kN. The displacement of deflection in the mid-span of G9 is the highest among the other specimens due to its smallest thickness of sheathing materials and having the least stiffness in resisting the vertical deflection caused by the constant applied load. In load bearing capacity test, G9 is capable to sustain the highest compressive load among the other specimens and experienced the largest displacement of lateral deflection due to its thickest RLFC core and thinnest sheathing material.

CHAPTER 5

CONCLUSION AND RECOMMENDATIONS

5.1 Conclusions

The practicality of using gypsum boards as the sheathing materials and rubberized lightweight foamed concrete (RLFC) as the inner core in a sized down composite sandwiched RLFC wall panel was studied by conducting flame exposure, thermal conductivity, flexural strength and load bearing capacity tests. The adhesive used in connecting the gypsum board and RLFC core to form a sandwiched wall panel was epoxy resin.

The first objective of this study is to investigate the structural reliability of sandwiched RLFC wall panels in terms of buckling performance. This objective is accomplished by concluding that sandwiched RLFC wall panels that utilized 9 mm gypsum boards as sheathing materials (G9) possessed the highest load bearing capacity and the largest displacement of lateral deflection among the other specimens which is 73.6 kN and 1.76 mm respectively. This is because the RLFC core sustained a higher compressive load than the gypsum boards. Besides, the larger thicknesses of the gypsum boards in sandwiched RLFC wall panels were stiffer and more capable of resisting the lateral deflection caused by the constant applied compressive load. Moreover, G9, G12 and G16 experienced crushing failure instead of buckling failure after conducting the load bearing capacity test. This is because the thicknesses of the gypsum boards used as the sheathing materials in all the specimens are sufficiently large and stiff to mitigate the buckling effect caused by the constant applied compressive load.

The second objective of this study is to investigate the flexural strength of sandwiched RLFC wall panels. This objective is accomplished by concluding that G9, G12 and G16 possessed a similar ultimate flexural strength which is 8 kN after the flexural strength test. Moreover, G9 experienced the largest displacement of vertical deflection in the mid-span among the other specimens which is 6.69 mm. This is because the thickness of gypsum boards used as sheathing materials in G9 is the smallest and it had the least stiffness to resist

the vertical deflection caused by the constant applied load. Therefore, a larger thickness of sheathing materials is stiffer and more effective in resisting the vertical deflection caused by the constant applied load. Hence, G16 outperformed G9 and G12 in the flexural strength test.

The third objective of this study is to investigate the thermal conductivity of sandwiched RLFC wall panels. This objective is accomplished by concluding that G9 possessed the lowest value of thermal conductivity among the other specimens which is $0.4676 \text{ Wm}^{-1}\text{K}^{-1}$. To rephrase it, G9 is the best thermal insulator. This is because the RLFC core's thickness of G9 is the largest and there are more air voids and rubber aggregates in the RLFC core across its thickness. The air voids and rubber aggregates in the RLFC core improve its thermal insulation by trapping heat energy absorbed from the hot plate and slowing down the rate of heat transfer to the cold plate. Moreover, the density of the sheathing material which is the gypsum board used in G9 is the lowest at 557.895 kg/m^3 among the other specimens. The higher the density of the gypsum boards, the lesser the void spaces and this increases the rate of heat transfer through the specimen from hot plate to cold plate resulting in the increase of thermal conductivity. Therefore, G9 outperformed G12 and G16 in the thermal conductivity test.

The last objective of this study is to investigate the fire performance of sandwiched RLFC wall panels. This objective is accomplished by concluding that G9, G12 and G16 possessed similar fire performance by having similar surface conditions after the flame exposure test. Moreover, the connection between the RLFC core and the sheathing materials as well as the structural integrity of the sandwiched RLFC wall panels were not compromised by the 60 minutes of continuous direct flame exposure. Therefore, the fire performance of the sandwiched wall panels was satisfactory as the specimens have proven their capability in providing effective fire protection against continuous flame exposure at an extreme temperature of $600 \text{ }^\circ\text{C}$ and above. Hence, gypsum boards are suitable sheathing materials utilized in a sandwich wall panel system to provide supreme fire protection.

5.2 Recommendations

The study of the structural performances and fire-resisting ability of rubberized lightweight foamed concrete (RLFC) wall panels with a density of 1150 kg/m^3 utilizing gypsum board as a skin layer is still limited in this field. The following recommendations and suggestions could be taken into account to enhance and produce more reliable and accurate results for future research:

1. Study the effects of various proportions of powdered rubber aggregate in RLFC core to have a better comparison in thermal conductivity, load bearing capacity, fire performance and flexural strength.
2. Study the effects of different types of rubber aggregate such as crumb rubber and powdered rubber aggregates utilized in RLFC core to have a better comparison in thermal conductivity, load bearing capacity, fire performance and flexural strength.
3. Various types of sheathing materials to be used in the sandwiched RLFC wall panel such as calcium silicate board and magnesium oxide board are recommended to have a better comparison in fire performance, thermal conductivity, flexural strength and load bearing capacity instead of having the same type of sheathing material which is gypsum board.
4. Investigate the effects of adding admixture such as zeolite into the RLFC core of the sandwiched wall panel on its flexural strength.
5. A lower rate of a constant applied load than 0.5 kN/s in the flexural strength test is recommended to obtain a more accurate result of the ultimate flexural strength of the sandwiched RLFC wall panels.

REFERENCES

- Abdullah, W. A., AbdulKadir, M. R. and Muhammad, M. A., 2018. Effect of High Temperature on Mechanical Properties of Rubberized Concrete Using Recycled Tire Rubber as Fine Aggregate Replacement. *Engineering and Technology Journal*, 36(8), pp.906-913.
- Agrawal, Y., Gupta, T., Sharma, R., Panwar, N. L. and Siddique, S., 2021. A comprehensive review on the performance of structural lightweight aggregate concrete for sustainable construction. *Construction Materials*, 1(1), pp.39-62.
- Alam, I. and Khattak, K., 2015. Use of Rubber as Aggregate in Concrete: A Review. *International Journal of Advanced Structures and Geotechnical Engineering*, 4(2), pp.92-96.
- Ariyanayagam, A. D. and Mahendran, M., 2017. Fire tests of non-load bearing light gauge steel frame walls lined with calcium silicate boards and gypsum plasterboards. *Thin-Walled Structures*, 115, pp.86-99.
- Ates, E., 2009. Optimization of Compression Strength by Granulometry and Change of Binder Rates in Epoxy and Polyester Resin Concrete. *Journal of Reinforced Plastics and Composites*, 28(2), pp.235-246.
- Bhandari, P., 2016. Evaluating Properties of Lightweight Sandwich Wall Panels. *International Journal for Scientific Research & Development*, 4(6), pp.175-178.
- Borri, A., Corradi, M., Sisti, R., Buratti, C., Belloni, E. and Moretti, E., 2016. Masonry wall panels retrofitted with thermal-insulating GFRP-reinforced jacketing. *Materials and Structures*, 49, pp.3957-3968.
- Chen, W., Ye, J., Bai, Y. and Zhao, X. L., 2012. Full-scale fire experiments on load-bearing cold-formed steel walls lined with different panels. *Journal of Constructional Steel Research*, 79, pp.242-254.

Chi, J. M., Huang, R., Yang, C. C. and Chang, J. J., 2003. Effect of aggregate properties on the strength and stiffness of lightweight concrete. *Cement & Concrete Composites*, 25, pp.197-205.

Chowaniec, A. and Ostrowski, K., 2018. Epoxy resin coatings modified with waste glass powder for sustainable construction. *Technical Transactions*, 115(8), pp.99-109.

Chylík, R., Trtík, T., Fládr, J. and Bílý, P., 2017. Mechanical properties and durability of crumb rubber concrete. *Materials Science and Engineering*, 236(1), pp.012093.

Courard, L., 2002. Evaluation of thermodynamic properties of concrete substrates and cement slurries modified with admixtures. *Materials and Structures*, 35, pp.149-155.

Ding, K., Wang, G. and Yin, W., 2013. Application of composite sandwich panels in construction engineering. *Applied Mechanics and Materials*, 291-294, pp.1172-1176.

Fadiel, A., Rifaie, F. A., Abu-Lebdeh, T. and Fini, E., 2014. Use of crumb rubber to improve thermal efficiency of cement-based materials. *American Journal of Engineering and Applied Sciences*, 7(1), pp.1-11.

Fu, Y. X., He, Z. X., Mo, D. C. and Lu, S. S., 2014. Thermal conductivity enhancement with different fillers for epoxy resin adhesives. *Applied Thermal Engineering*, 66(2), pp.493-498.

Ganjan, E., Khorami, M. and Maghsoudi, A. A., 2009. Scrap-tyre-rubber replacement for aggregate and filler in concrete. *Construction and Building Materials*, 23(5), pp.1828-1836.

Grinys, A., Balamurugan, M., Augonis, A. and Ivanauskas, E., 2021. Mechanical properties and durability of rubberized and glass powder modified rubberized concrete for whitetopping structures. *Materials*, 14(9), pp.2321.

Gualtieri, M., Andrioletti, M., Vismara, C., Milani, M. and Camatini, M., 2005. Toxicity of tire debris leachates. *Environment International*, 31, pp.723–730.

Hernández-Olivares, F. and Barluenga, G., 2004. Fire performance of recycled rubber-filled high-strength concrete. *Cement and concrete research*, [e-journal] 34(1), pp.109-117. [https://doi.org/10.1016/S0008-8846\(03\)00253-9](https://doi.org/10.1016/S0008-8846(03)00253-9).

Jhatial, A. A., Goh, W. I., Mohamad, N., Rind, T. A. and Sandhu, A. R., 2020. Development of thermal insulating lightweight foamed concrete reinforced with polypropylene fibres. *Arabian Journal for Science and Engineering*, 45(5), pp.4067-4076.

Jokar, F., Khorram, M., Karimi, G. and Hataf, N., 2019. Experimental investigation of mechanical properties of crumbed rubber concrete containing natural zeolite. *Construction and Building Materials*, [e-journal] 208, pp.651-658. <https://doi.org/10.1016/j.conbuildmat.2019.03.063>.

Jones, M.R. and McCarthy, A., 2015. Behaviour and assessment of foamed concrete for construction applications. *ICE Virtual Library* [online]. Available at: <<https://www.icevirtuallibrary.com/doi/abs/10.1680/uofcic.34068.0008>> [Accessed: 2nd March 2022].

Júlio, E. N. B. S., Branco, F. A. B. and Silva, V. D., 2004. Concrete-to-concrete bond strength. Influence of the roughness of the substrate surface. *Construction and Building Materials*, 18(9), pp.675-681.

Khan, R. B. N. and Khitab, A., 2020. Enhancing Physical, Mechanical and Thermal Properties of Rubberized Concrete. *Engineering and Technology Quarterly Reviews*, 3(1), pp.33-47.

Kozłowski, M. and Kadela, M., 2018. Mechanical Characterization of Lightweight Foamed Concrete. *Advances in Materials Science and Engineering*, [e-journal] 2018, pp.1-8. <https://doi.org/10.1155/2018/6801258>.

Kumar, S., Chen, B., Xu, Y. and Dai, J. G., 2021. Structural behavior of FRP grid reinforced geopolymer concrete sandwich wall panels subjected to concentric axial loading. *Composite Structures*, 270, pp.114117.

Lakshmikandhan, K. N., Harshavardhan, B. S., Prabakar, J. and Saibabu, S., 2017. Investigation on Wall Panel Sandwiched with Lightweight Concrete. *Materials Science and Engineering*, 225(1), pp.012275.

Li, L. –J., Xie, W. –F., Liu, F., Guo, Y. –C. and Deng, J., 2011. Fire performance of high-strength concrete reinforced with recycled rubber particles. *Magazine of Concrete Research*, 63(3), pp.187-195.

Li, Y., Zhang, S., Wang, R. and Dang, F., 2019. Potential use of waste tire rubber as aggregate in cement concrete – A comprehensive review. *Construction and Building Materials*, [e-journal] 225, pp.1183-1201. <https://doi.org/10.1016/j.conbuildmat.2019.07.198>.

Lim, S. K., Tan, C. S., Lim, O. Y. and Lee, Y. L., 2013. Fresh and hardened properties of lightweight foamed concrete with palm oil fuel ash as filler. *Construction and Building Materials*, 46, pp.39-47.

Lo, T. Y., Cui, H. Z. and Li, Z. G., 2004. Influence of aggregate pre-wetting and fly ash on mechanical properties of lightweight concrete. *Waste Management*, 24, pp.333-338.

Lo, T. Y., Tang, W. C. and Cui, H. Z., 2007. The effects of aggregate properties on lightweight concrete. *Building and Environment*, 42, pp.3025-3029.

Marie, I., 2017. Thermal conductivity of hybrid recycled aggregate – Rubberized concrete. *Construction and Building Materials*, 133, pp.516-524.

Mohajerani, A., Burnett, L., Smith, J.V., Markovski, S., Rodwell, G., Rahman, M.T., Kurmus, H., Mirzababaei, M., Arulrajah, A., Horpibulsuk, S. and Maghool, F., 2020. Recycling waste rubber tyres in construction materials and

associated environmental considerations: A review. *Resources, Conservation and Recycling*, 155, pp.104679.

Muhammad, M. A., Abdullah, W. A. and Abdul-Kadir, M. R., 2017. Post-fire mechanical properties of concrete made with recycled tire rubber as fine aggregate replacement. *Sulaimania Journal for Engineering Sciences*, 4(5), pp.74-85.

Newman, J. and Owens, P., 2003. 2 - Properties of lightweight concrete. *Advanced Concrete Technology*, [e-journal] 4, pp.3-29. <https://doi.org/10.1016/B978-075065686-3/50288-3>.

Park, S. H., Manzello, S. L., Bentz, D. P. and Mizukami, T., 2009. Determining thermal properties of gypsum board at elevated temperatures. *Fire and Materials*, 34(5), pp.237-250.

Rahman, A. K. M. L., Barai, A., Sarker, A. and Moniruzzaman, M., 2018. Light weight concrete from rice husk ash and glass powder. *Bangladesh Journal of Scientific and Industrial Research*, 53(3), pp.225-232.

Rahmanian, I. and Wang, Y. C., 2012. A combined experimental and numerical method for extracting temperature-dependent thermal conductivity of gypsum boards. *Construction and Building Materials*, [e-journal] 26(1), pp.707-722. <https://doi.org/10.1016/j.conbuildmat.2011.06.078>.

Shakya, P. R., Shrestha, P., Tamrakar, C. S. and Bhattarai, P. K., 2006. Studies and determination of heavy metals in waste tyres and their impacts on the environment. *Pakistan Journal of Analytical & Environmental Chemistry*, 7(2), pp.70-76.

Simonetti, C., Tutikian, B. F. and da Silva Filho, L. C. P., 2021. Fire Resistance of Concrete Panels Made with Recycled Tire Materials. *ACI Materials Journal*, 118(5), pp.173-184.

Singh, A., Spak, S. N., Stone, E. A., Downard, J., Bullard, R. L., Pooley, M., Kostle, P. A., Mainprize, M. W., Wichman, M. D., Peters, T. M. and Beardsley, D., 2015. Uncontrolled combustion of shredded tires in a landfill–Part 2: Population exposure, public health response, and an air quality index for urban fires. *Atmospheric Environment*, 104, pp.273-283.

Talebi, H. R., Kayan, B. A., Asadi, I. and Hassan, Z. F. A., 2020. Investigation of Thermal Properties of Normal Weight Concrete for Different Strength Classes. *Journal of Environmental Treatment Techniques*, 8(3), pp.908-914.

Wakili, K. G., Hugi, E., Wullschleger and Frank, T., 2006. Gypsum Board in Fire – Modeling and Experimental Validation. *Journal of Fire Sciences*, 25(3), pp.267-282.

Weber, B., 2012. Heat transfer mechanisms and models for a gypsum board exposed to fire. *International Journal of Heat and Mass Transfer*, 55(5-6), pp.1661-1678.

Yu, Q. L. and Brouwers, H. J. H., 2011. Thermal properties and microstructure of gypsum board and its dehydration products: A theoretical and experimental investigation. *Fire and Materials*, [e-journal] 36(7), pp.575-589. <https://doi.org/10.1002/fam.1117>.

Zhou, A., Wong, K. W. and Lau, D., 2014. Thermal Insulating Concrete Wall Panel Design for Sustainable Built Environment. *The Scientific World Journal*, [e-journal] 2014, pp.1-12. <https://doi.org/10.1155/2014/279592>.